# General Disclaimer

## One or more of the Following Statements may affect this Document

- This document has been reproduced from the best copy furnished by the organizational source. It is being released in the interest of making available as much information as possible.

- This document may contain data, which exceeds the sheet parameters. It was furnished in this condition by the organizational source and is the best copy available.

- This document may contain tone-on-tone or color graphs, charts and/or pictures, which have been reproduced in black and white.

- This document is paginated as submitted by the original source.

- Portions of this document are not fully legible due to the historical nature of some of the material. However, it is the best reproduction available from the original submission.

# NASA TECHNICAL MEMORANDUM

NASA TM-78166

(NASA-TM-78166) SOLAR ACTIVITY DURING SKYLAB: ITS DISTRIBUTION AND RELATION TO CORONAL HOLES (NASA) 35 p HC A03/MF A01 CSCL 03B

N78-22994

Unclas

G3/92 15671

## SOLAR ACTIVITY DURING SKYLAB – ITS DISTRIBUTION AND RELATION TO CORONAL HOLES

By David M. Speich, Jesse B. Smith, Jr., Robert M. Wilson, and Patrick S. McIntosh

April 1978

NASA

*George C. Marshall Space Flight Center*
*Marshall Space Flight Center, Alabama*

TECHNICAL REPORT STANDARD TITLE PAGE

| | | |
|---|---|---|
| 1. REPORT NO. NASA TM-78166 | 2. GOVERNMENT ACCESSION NO. | 3. RECIPIENT'S CATALOG NO. |
| 4. TITLE AND SUBTITLE Solar Activity During Skylab — Its Distribution and Relation to Coronal Holes | | 5. REPORT DATE April 1978 |
| | | 6. PERFORMING ORGANIZATION CODE |
| 7. AUTHOR(S) David M. Speich,* Jesse B. Smith, Jr.,* Robert M. Wilson, and Patrick S. McIntosh** | | 8. PERFORMING ORGANIZATION REPORT # |
| 9. PERFORMING ORGANIZATION NAME AND ADDRESS George C. Marshall Space Flight Center Marshall Space Flight Center, Alabama 35812 | | 10. WORK UNIT NO. |
| | | 11. CONTRACT OR GRANT NO. |
| | | 13. TYPE OF REPORT & PERIOD COVERED Technical Memorandum |
| 12. SPONSORING AGENCY NAME AND ADDRESS National Aeronautics and Space Administration Washington, D.C. 20546 | | |
| | | 14. SPONSORING AGENCY CODE |

15. SUPPLEMENTARY NOTES
Prepared by Space Sciences Laboratory, Science and Engineering
*NOAA SEL SESC, currently located at Marshall Space Flight Center
**NOAA SEL SESC, Boulder, Colorado 80302

16. ABSTRACT

Solar active regions observed during the period of Skylab observations (May 1973–February 1974) have been examined for properties that varied systematically with location on the Sun, particularly with respect to the location of coronal holes. Approximately 90 percent of the optical and X-ray flare activity occurred in one solar hemisphere (136–315 heliographic degrees longitude). Active regions within 20 heliographic degrees of coronal holes were below average in lifetimes, flare production, and magnetic complexity. Histograms of solar flares as a function of solar longitude have been aligned with Hα synoptic charts on which active region serial numbers and coronal hole boundaries have been added.

| | |
|---|---|
| 17. KEY WORDS | 18. DISTRIBUTION STATEMENT Unclassified – Unlimited Jesse Smith |

| 19. SECURITY CLASSIF. (of this report) | 20. SECURITY CLASSIF. (of this page) | 21. NO. OF PAGES | 22. PRICE |
|---|---|---|---|
| Unclassified | Unclassified | 25 | |

MSFC - Form 3292 (Rev December 1972)    For sale by National Technical Information Service, Springfield, Virginia 22151

## ACKNOWLEDGMENTS

One of the authors (David M. Speich) wishes to acknowledge the efforts of the NOAA solar forecasters during the Skylab missions. A significant amount of the analysis presented in this report was performed and presented to the Skylab solar experimenters in real time. This work was performed, in part, in support of the Skylab Solar Workshop Series. Part of this work was supported by Skylab data analysis funds (Government Work Order H-12261-B, NASA, MSFC).

# TABLE OF CONTENTS

# LIST OF ILLUSTRATIONS

# LIST OF ILLUSTRATIONS (Concluded)

TECHNICAL MEMORANDUM

# SOLAR ACTIVITY DURING SKYLAB – ITS DISTRIBUTION AND RELATION TO CORONAL HOLES

## INTRODUCTION

In the course of assembling the record of solar activity during the period of Skylab observations, researchers have noted that solar flares [1], sunspots and coronal transients [2], and coronal bright points [3] were not distributed uniformly in solar longitude but, instead, were associated with one hemisphere of the Sun (136-315 heliographic degrees longitude). In contrast, coronal holes dominated the quiet hemisphere [1,4]. In this report, we examine the distribution and properties of solar active regions observed during the Skylab period, comparing regions within the active hemisphere with regions near coronal holes.

Correlations are presented of (1) flare activity versus heliographic longitude, (2) active region lifetimes versus coronal hole proximity, (3) active region flare production versus coronal hole proximity, and (4) active region magnetic configurations versus coronal hole proximity. Also presented are H$\alpha$ synoptic maps showing coronal hole outlines, each map including an activity histogram for each Carrington rotation and a chart summarizing solar activity for the entire Skylab mission period.

## METHODOLOGY

Solar activity during the Skylab period is shown in Figures 1 through 10, using histograms and H$\alpha$ synoptic charts. The charts are annotated with the serial numbers of active regions and filaments as assigned by the National Oceanic and Atmospheric Administration's (NOAA) Space Environment Center in Boulder, Colorado. Furthermore, these charts identify the neutral lines in the radial component of the solar magnetic fields as mapped by filaments and systems of fine structures visible in H$\alpha$ filtergrams obtained by flare patrol telescopes [5]. Bohlin [4], Bohlin and Rubenstein [6], and McIntosh et al. [7] have shown that the boundaries of coronal holes have a close relationship to the patterns of large-scale magnetic fields as depicted from H$\alpha$ observations. To these charts we have added the coronal hole outlines as published by Nolte et al. [8] and Bohlin and Rubenstein [6].

Active regions $\leq 20$ degrees from any coronal hole boundary were utilized in the coronal hole/active region study. These distances were measured from the centroid of the H$\alpha$ region to the border of the coronal hole (at central meridian) as depicted on the synoptic maps.

H$\alpha$ flare activity during Skylab was tabulated by the NOAA/Air Weather Service (AWS) real-time solar observing network, subsequent film reviews, and by other solar observatories. Interpretation and compilation of these reports were performed by Hirman et al. [9]. X-ray flare magnitudes were determined from SOLRAD 9 and VELA satellite observations. Using these H$\alpha$ and X-ray data, we have plotted the distribution of solar flare occurrence versus heliographic longitude in 5 degree increments for each rotation (shown in Figures 1 through 10 below the synoptic maps as histograms). Figure 11 illustrates flare occurrence versus heliographic longitude and active region positions for the entire Skylab period. (Only flare activity observed during the Skylab mission is included in Figure 11.)

Lifetimes of active regions were determined by their appearance and disappearance as depicted on inferred magnetic neutral line maps which were drawn in real time from H$\alpha$ prints transmitted (approximately every 8 hours) to the NOAA solar support group at the NASA/Johnson Space Center. Active region lifetimes in days (t) were divided into three groups: $t \leq 1$, $1 < t \leq 7$, and $t > 7$. Active regions which traversed the east limb and died on the disk within 7 days and those which were born on the disk and then traversed the west limb within 7 days are included in this sample. However, since their lifetimes are somewhat ambiguous, we have assigned half of these regions to the second group ($1 < t \leq 7$) and half to the third group ($t > 7$).

Comparison of active region magnetic parameters was achieved utilizing Mt. Wilson's classification system and data. For NOAA active regions with corresponding Mt. Wilson region numbers, the maximum magnetic complexity observed was taken from the Solar Geophysical Data (Prompt) region reports. For NOAA active regions without corresponding Mt. Wilson region numbers, NOAA/AWS observatory determinations of Mt. Wilson classifications were used. These parameters were subdivided into three subsets of increasing complexity: (1) regions without sunspots, (2) regions with Mt. Wilson classification of $\alpha$ or $\beta$, and (3) regions with Mt. Wilson classification of $\beta\gamma$ or $\beta\gamma\Delta$.

# ANALYSIS

As Dodson and Hedeman [1] reported, the Sun exhibited an active and an inactive hemisphere during the Skylab mission period from mid-1973 to mid-1974. As shown in Figure 11, the active hemisphere was actually comprised of three discrete, active longitude bands: 145-175 degrees, 185-220 degrees, and 240-295 degrees. Table 1 and Figure 12 present the flare production for the active hemisphere. Although only 59 percent of the total number of regions observed during Skylab lay in this active hemisphere, they accounted for approximately 90 percent of the total number of flares.

Table 1 and Figure 12 also show the activity produced by active regions ≤ 20 degrees from the coronal holes. One finds that the optical and X-ray flare production by these regions is less per region when compared to the regions associated with the active hemisphere. Furthermore, when the larger optical or more energetic X-ray flares are considered, flare production per region is lower still. For those regions measured to be ≤ 10 degrees from a coronal hole boundary (14 percent of the toal number of regions), we find that flare production is decreased to approximately 10 percent of the Skylab total. (In Figure 12a, percentages for regions near coronal holes reflect the percentage of total flare production of those regions after normalization of the number of the coronal hole regions to the number of active hemisphere regions.)

Included in this sample of regions ≤ 10 degrees from a coronal hole is a flare-rich active complex composed of regions 287 and 292. Coronal hole 2* [10] formed approximately 5 degrees from these two regions during rotation 1608. The location of regions 287 and 292 became exceedingly quiet during the subsequent two solar rotations, producing only one subflare, while coronal hole 2* enlarged and became connected to the southern polar hole. While the location of regions 287 and 292 is within one of the active longitude belts, the development of coronal hole 2* appears to have effected the subsequent damping of the flare production of that previously active area. The appearance of active regions 287 and 292 in that active longitude band is not anomalous. The resultant effects of the subsequent birth and growth of coronal hole 2* are believed part of a large-scale, long-lived process rather than the effects of individual active region parameters.

The contribution of active regions 287 and 292 to the flare production totals of regions ≤ 10 degrees from coronal holes is significant. Without that contribution, the remaining 31 regions (13 percent of the total) ≤ 10 degrees from coronal holes produced only 2 percent of the total subflare production with no X-ray flares exceeding the class C intensity being observed.

Because of the expanded active region numbering scheme used by solar forecasters during Skylab,[1] there is an inherent bias toward a higher number of small, short-lived active regions in this study as compared to most previous studies of active region lifetimes defined by sunspot and calcium plage parameters. However, since forecaster adherence to the criteria for assignment of region numbers remained consistent within the Skylab period, numbered active regions can be compared and correlated by longitudinal distribution within that period.

From Table 1 and Figure 12b we note that the active hemisphere contained more long- than short-lived active regions. We also note that the converse of this is true for active regions in the vicinity of coronal holes.

Finally, in Table 1 and Figure 12c, Mt. Wilson magnetic classifications for Skylab active regions are compared. Regions in the active longitudes had a tendency to be more complex than average, and regions near coronal holes were slightly less complex. In fact, for the subset of active regions $\leq 10$ degrees from coronal holes (excluding regions 287 and 292) no complex magnetic configurations were observed. The percentage of normal and reversed polarity regions for the different subsets of active regions is approximately equal to that of the whole Sun.

## CONCLUSIONS

Based upon this study of a discrete portion of a solar cycle, several trends become evident. During Skylab, active regions near coronal holes generally (1) produced very little flare activity, (2) had relatively short lifetimes, and (3) were magnetically simple. Also during Skylab, the Sun contained an active hemisphere which (1) was composed of three distinct longitude bands of activity and (2) produced almost all of the flaring activity.

1. The criteria for assigning a NOAA region number to an H$\alpha$ feature during Skylab differed somewhat from those generally used prior and subsequent to Skylab. In addition to regions with sunspots and those which produced flares, emerging flux regions and other regions of specific interest to the Skylab solar experimenters were also given region numbers.

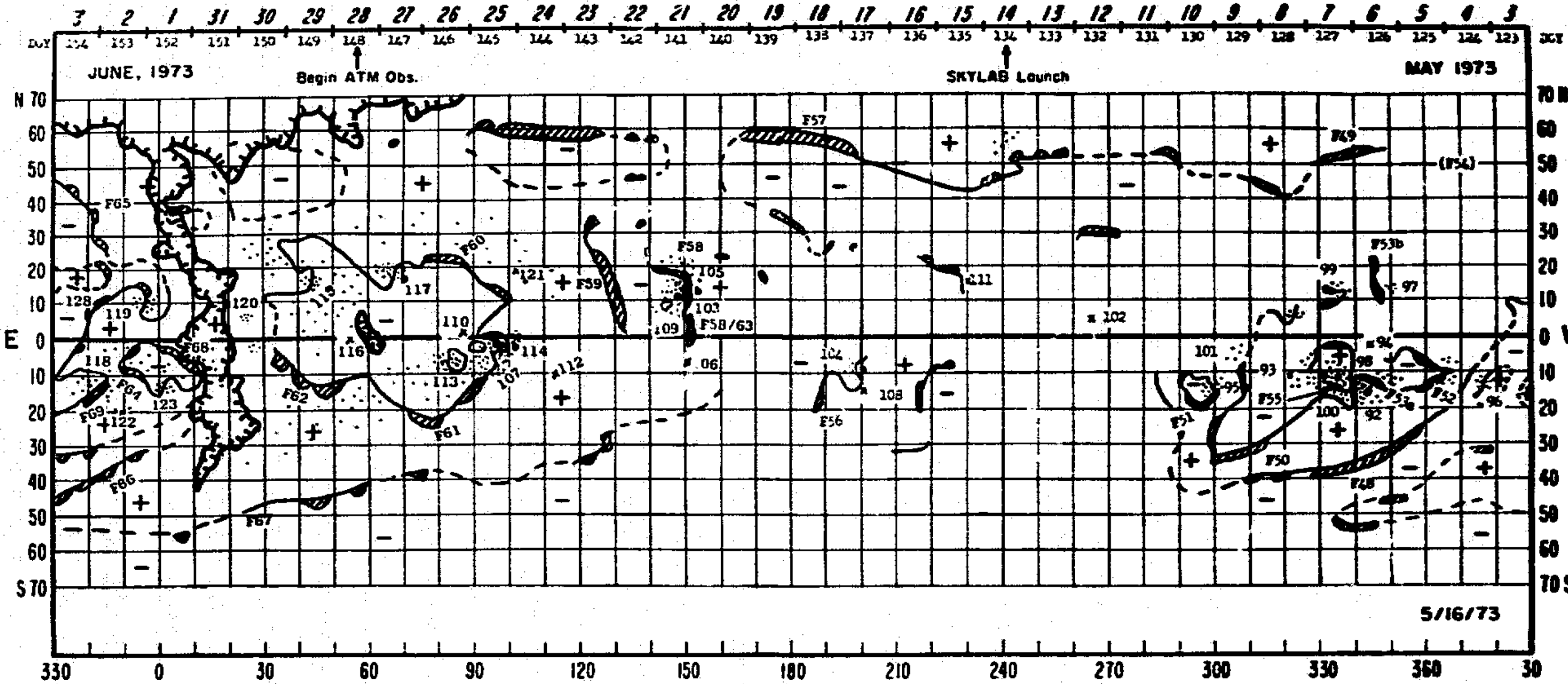


ROTATION NO. 1601 (MAY 5 - JUNE 1)

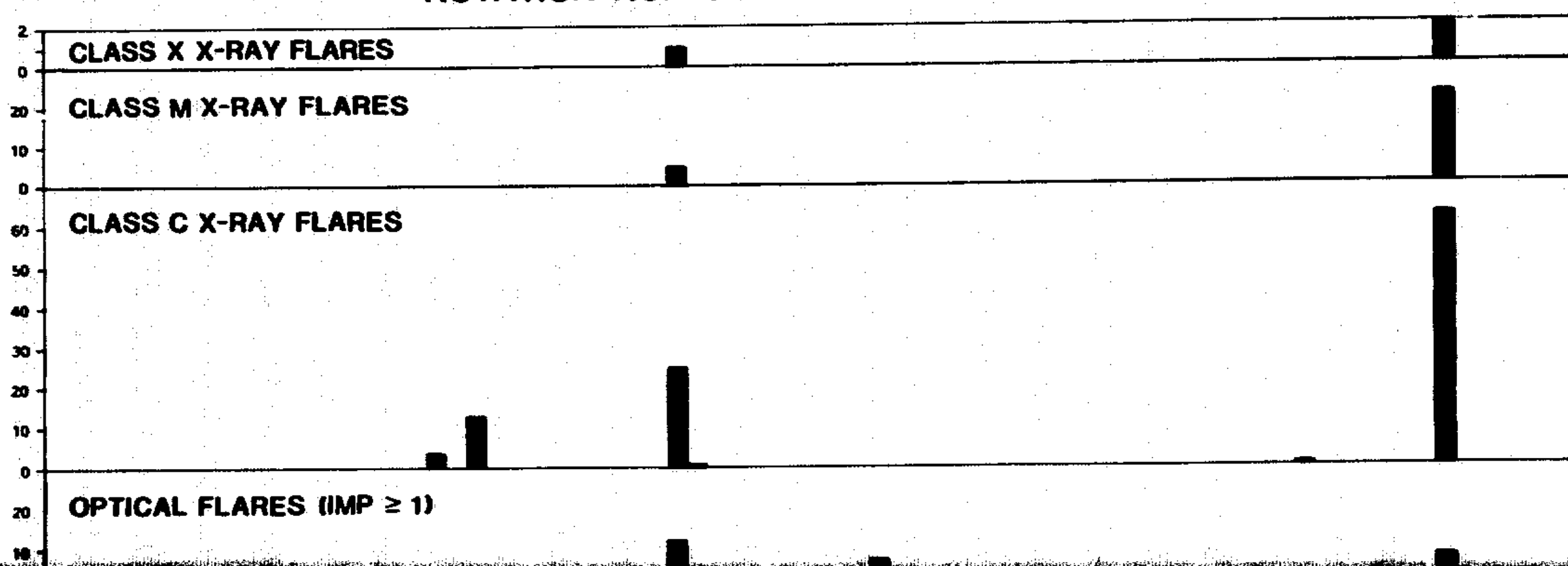


FOLDOUT FRAME

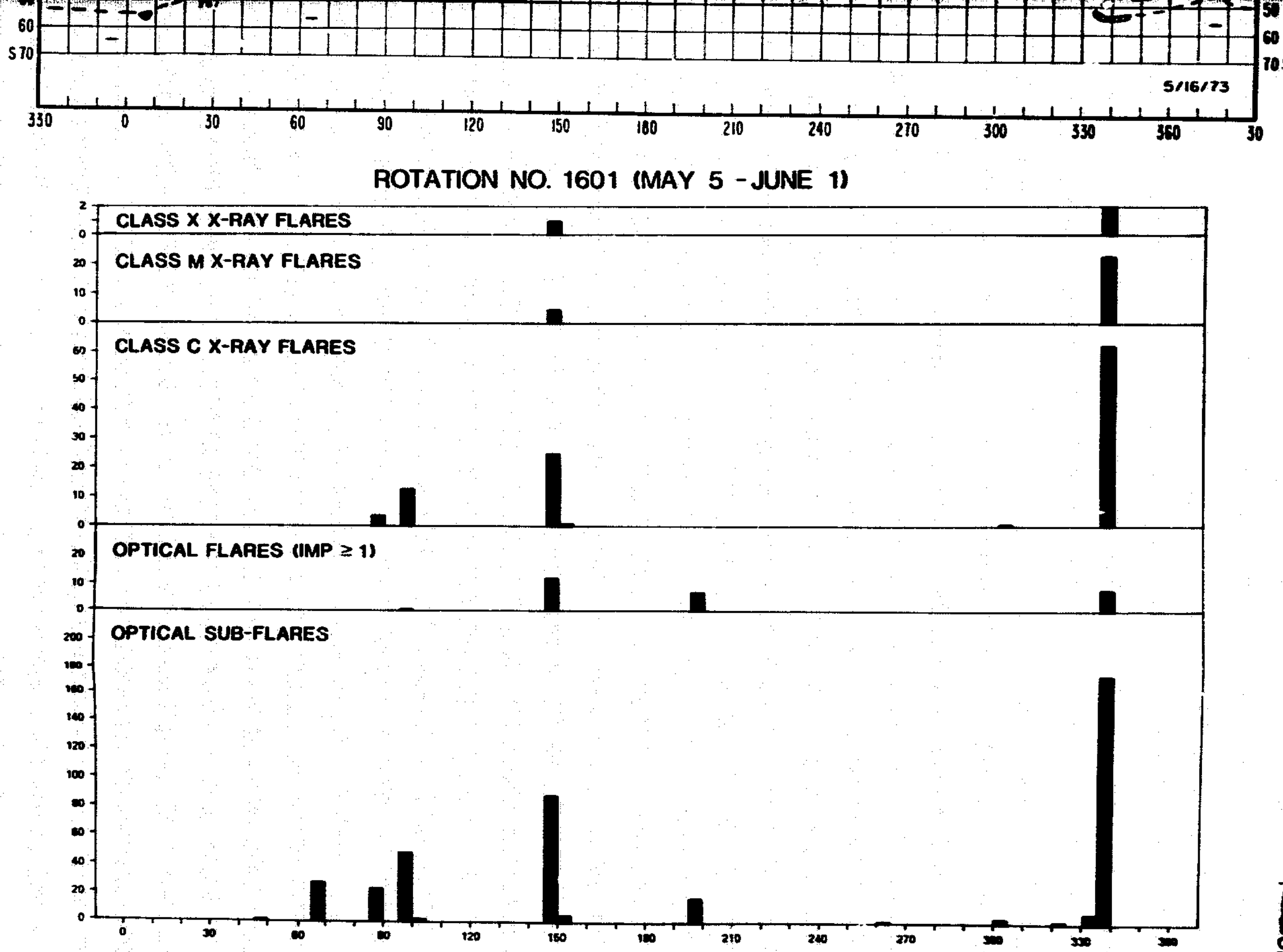


Figure 1. Hα synoptic chart with coronal hole boundaries aligned with flare activity histogram for Carrington rotation 1601.

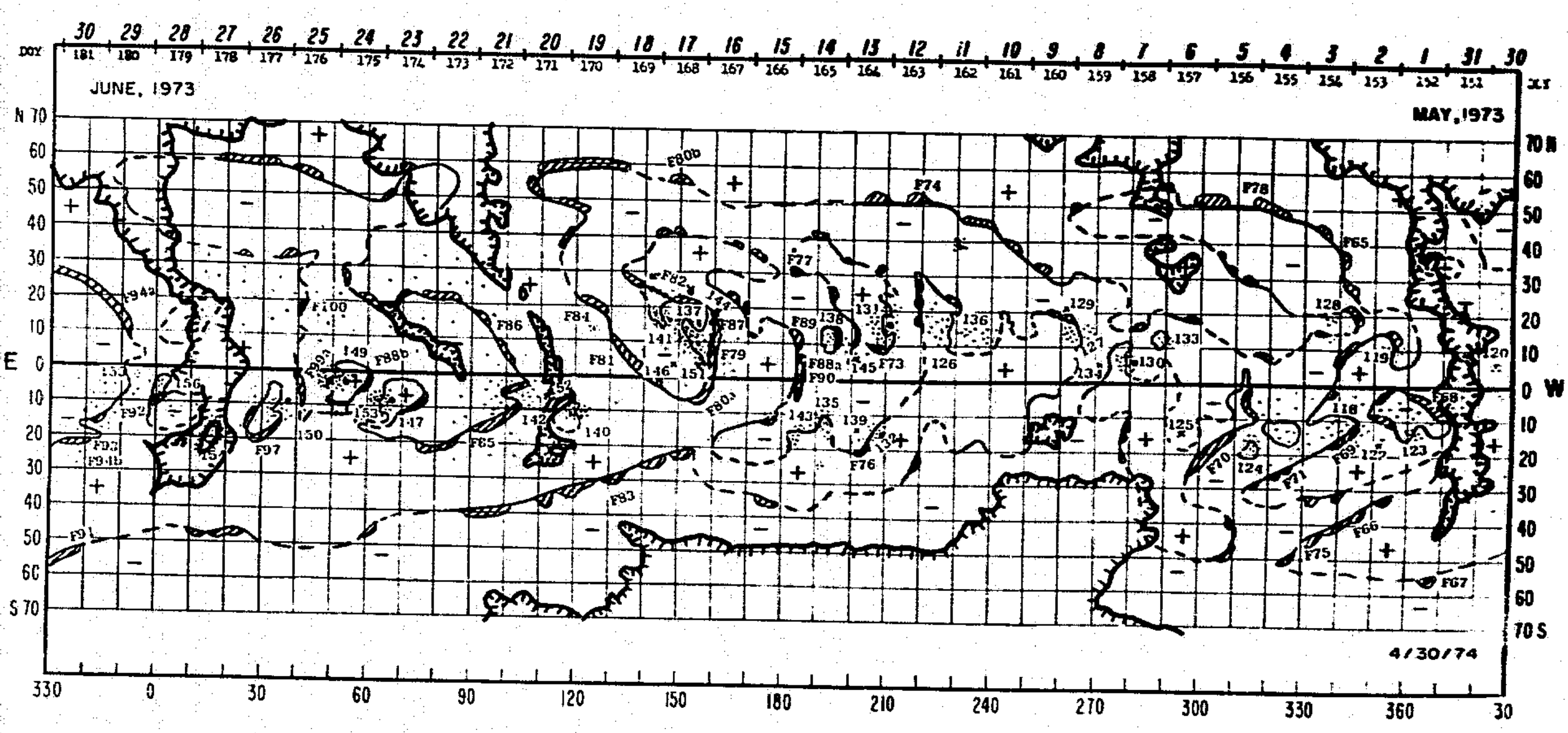


ROTATION NO. 1602 (JUNE 1 - JUNE 28)

CLASS X X-RAY FLARES

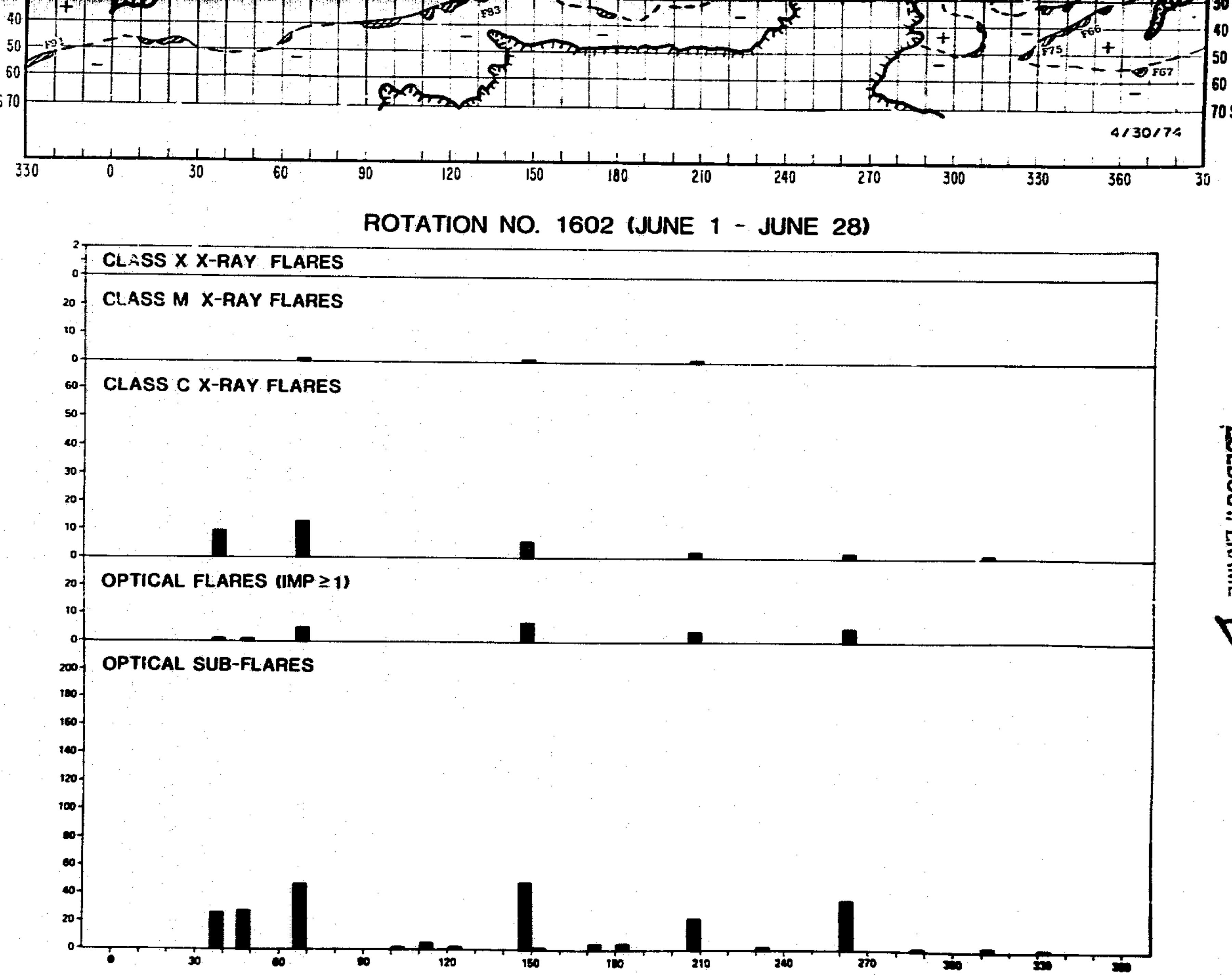


Figure 2. Hα synoptic chart with coronal hole boundaries aligned with flare activity histogram for Carrington rotation 1602.

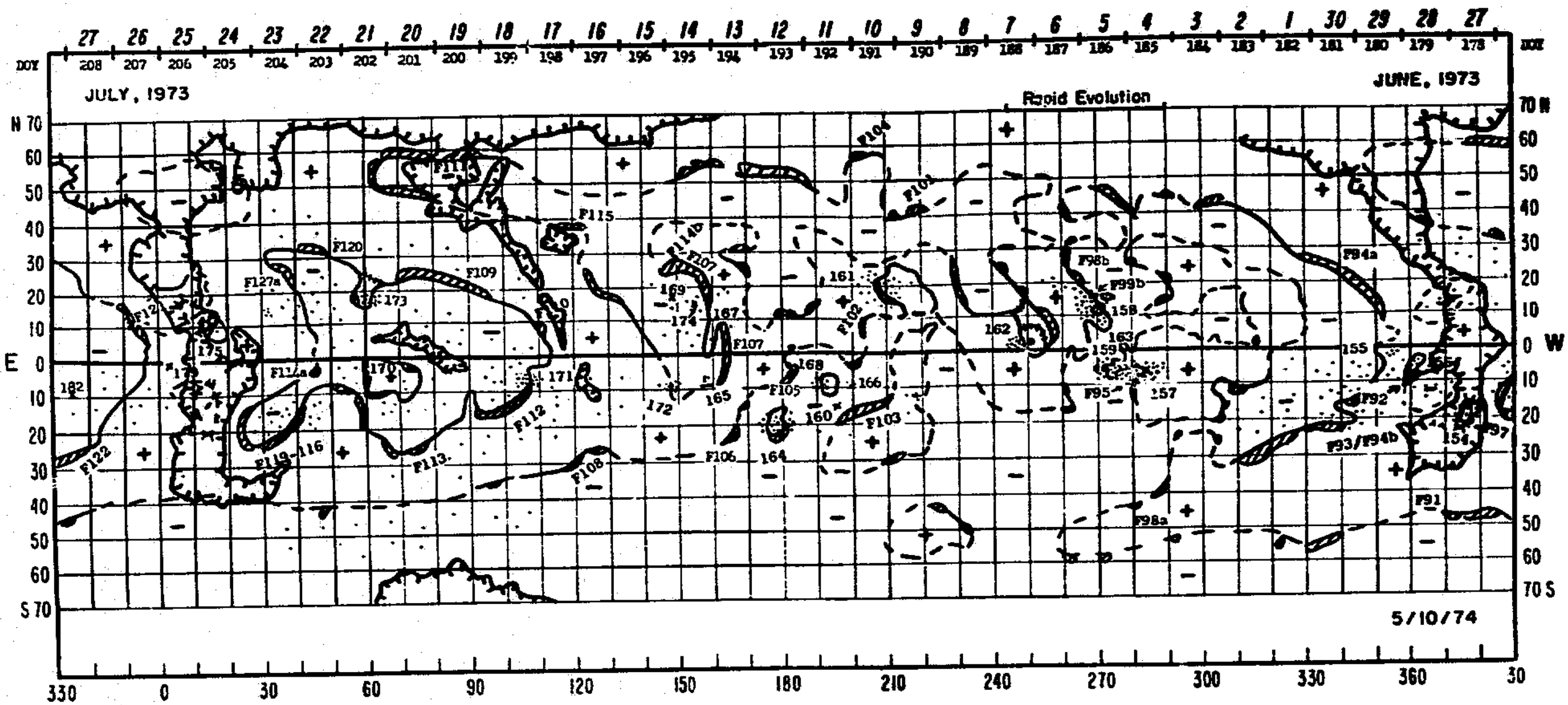


## ROTATION NO. 1603 (JUNE 28 - JULY 26)

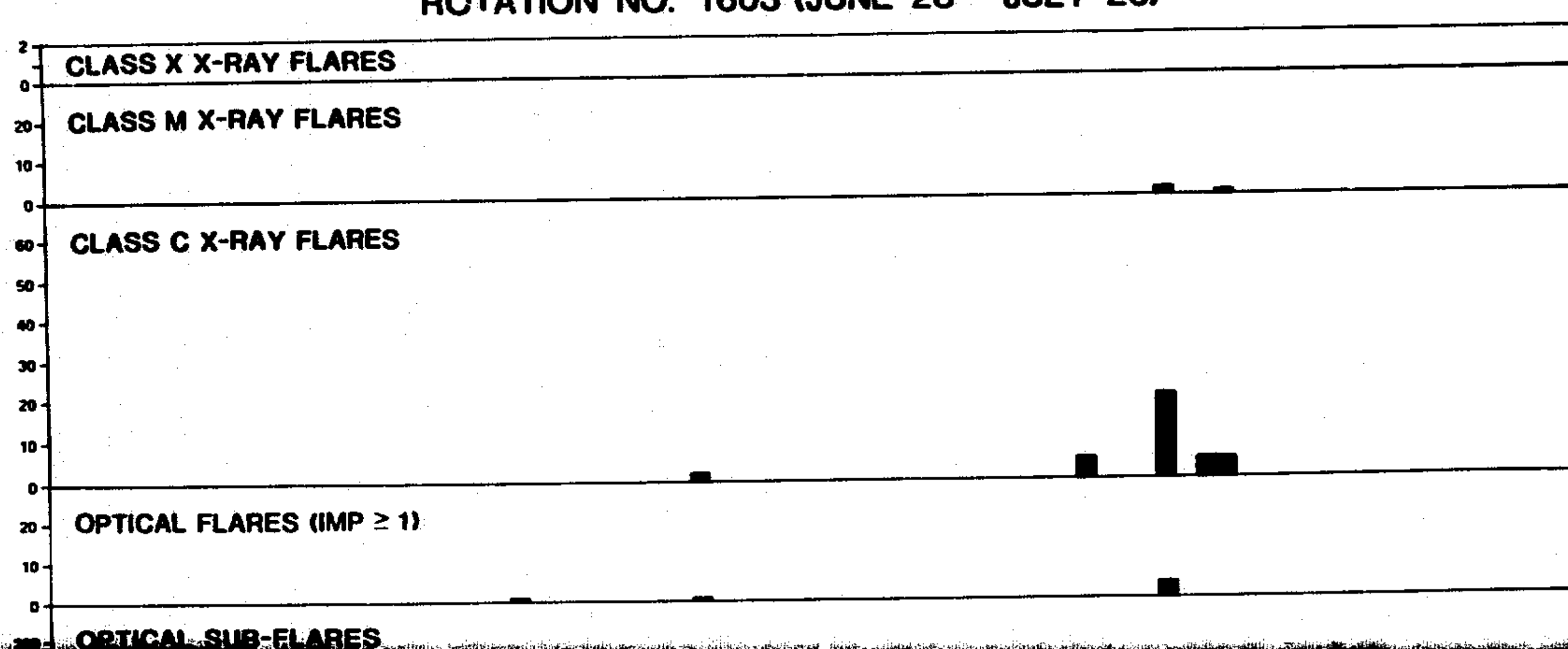


FOLDOUT FRAME

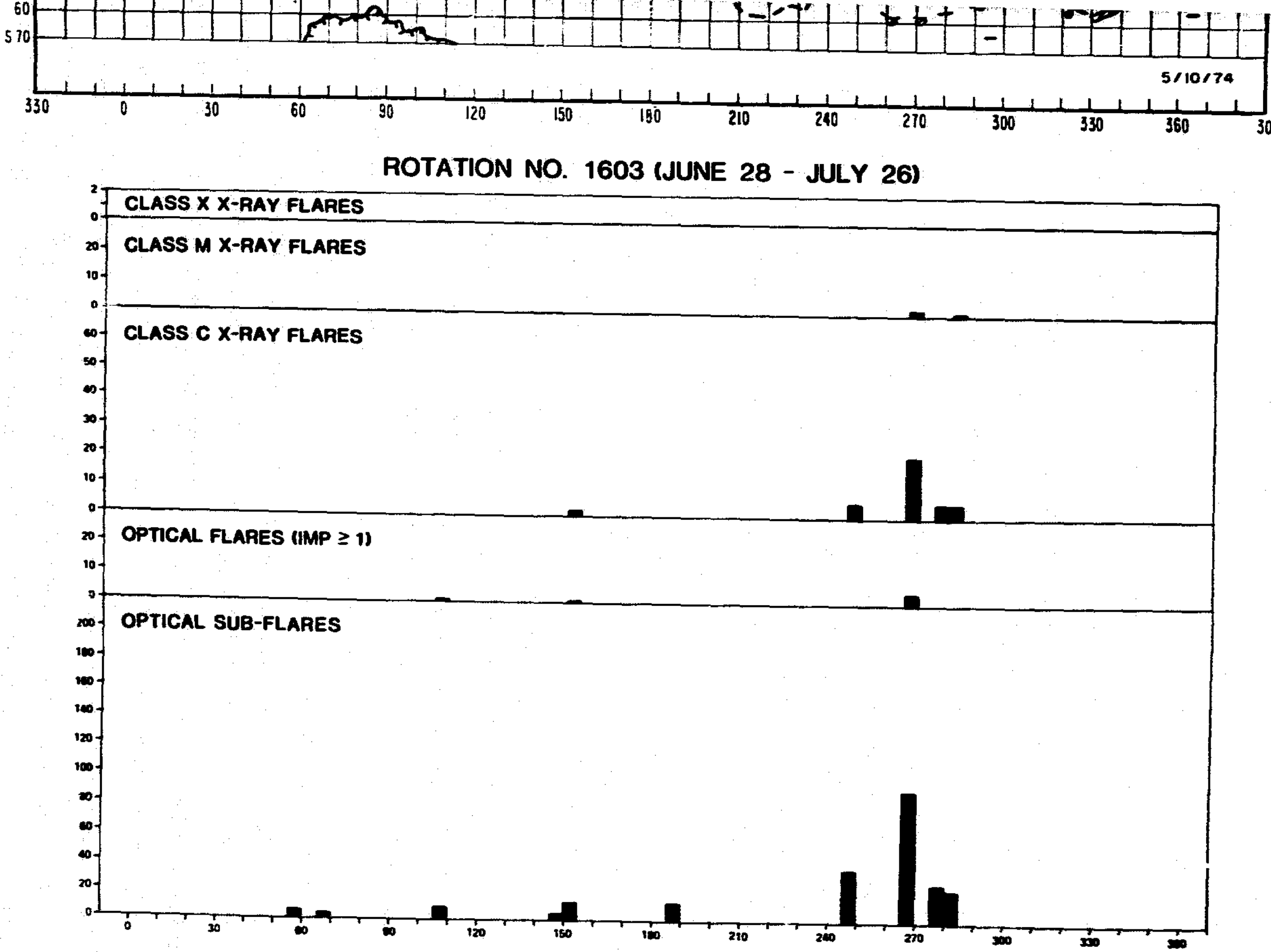


Figure 3. Hα synoptic chart with coronal hole boundaries aligned with flare activity histogram for Carrington rotation 1603.

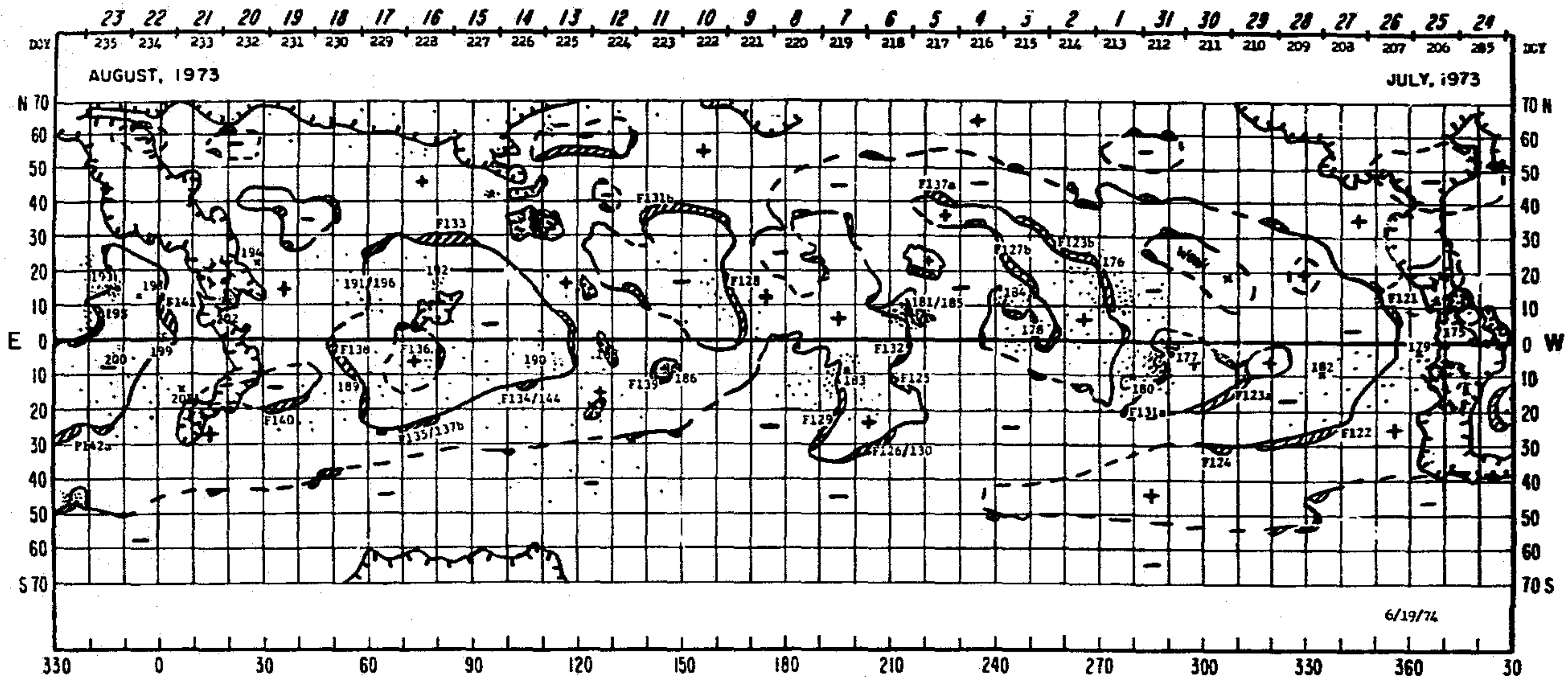


ROTATION NO. 1604 (JULY 26 - AUGUST 22)

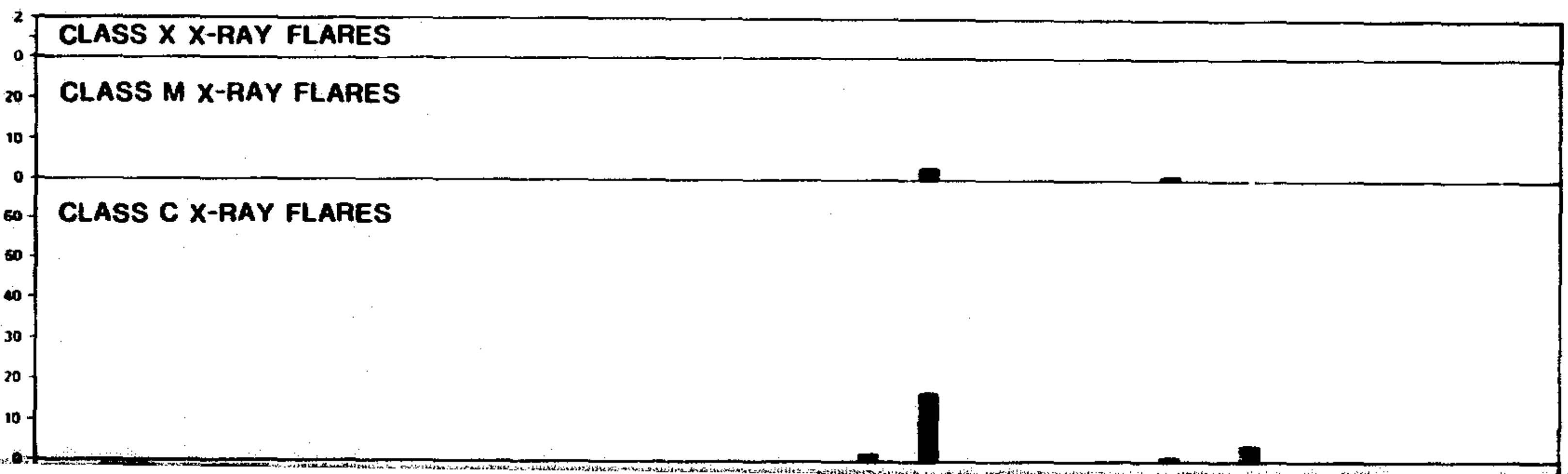


FOLDOUT FRAME

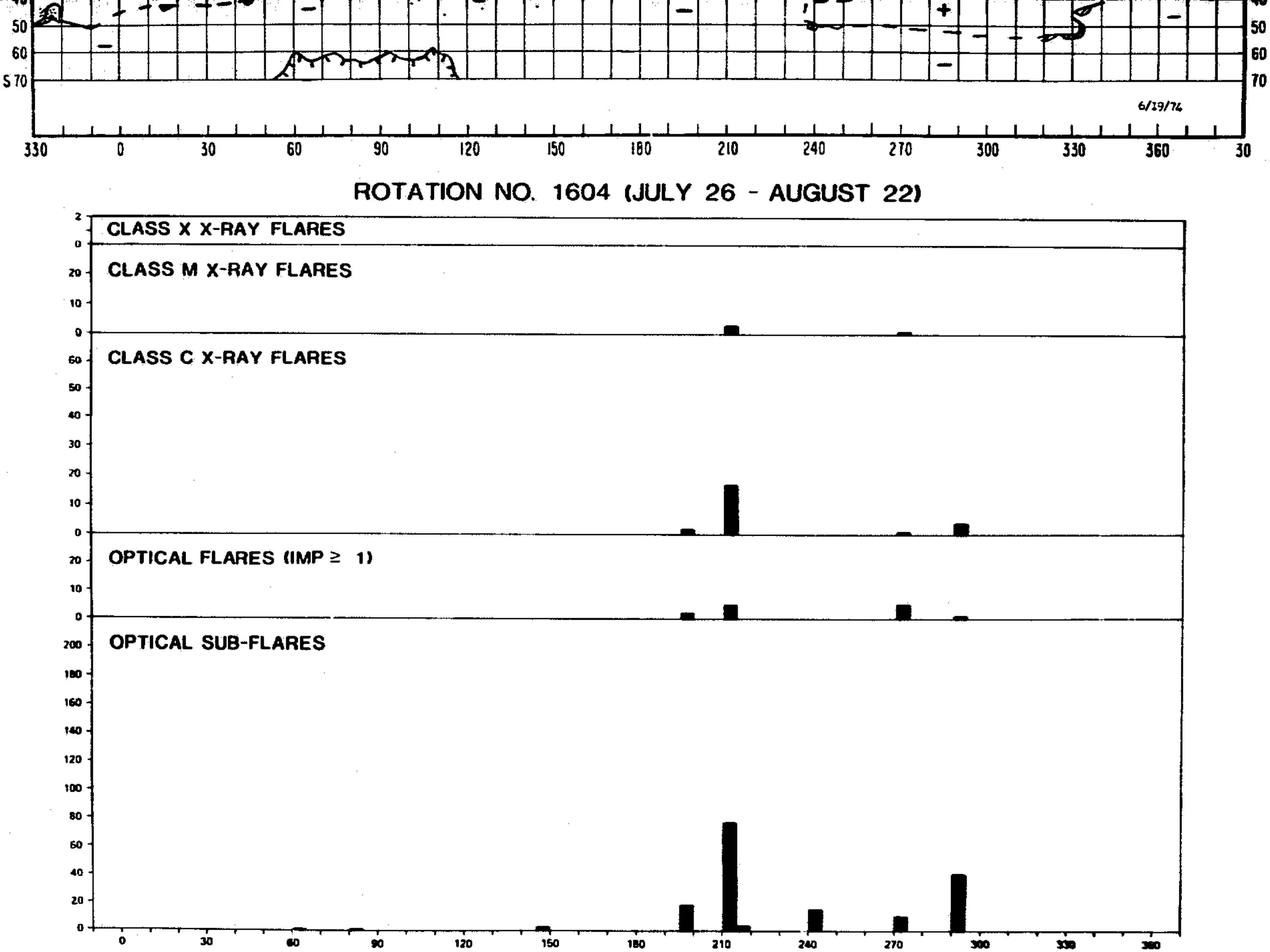


FOLDOUT FRAME 2

Figure 4. Hα synoptic chart with coronal hole boundaries aligned with flare activity histogram for Carrington rotation 1604.

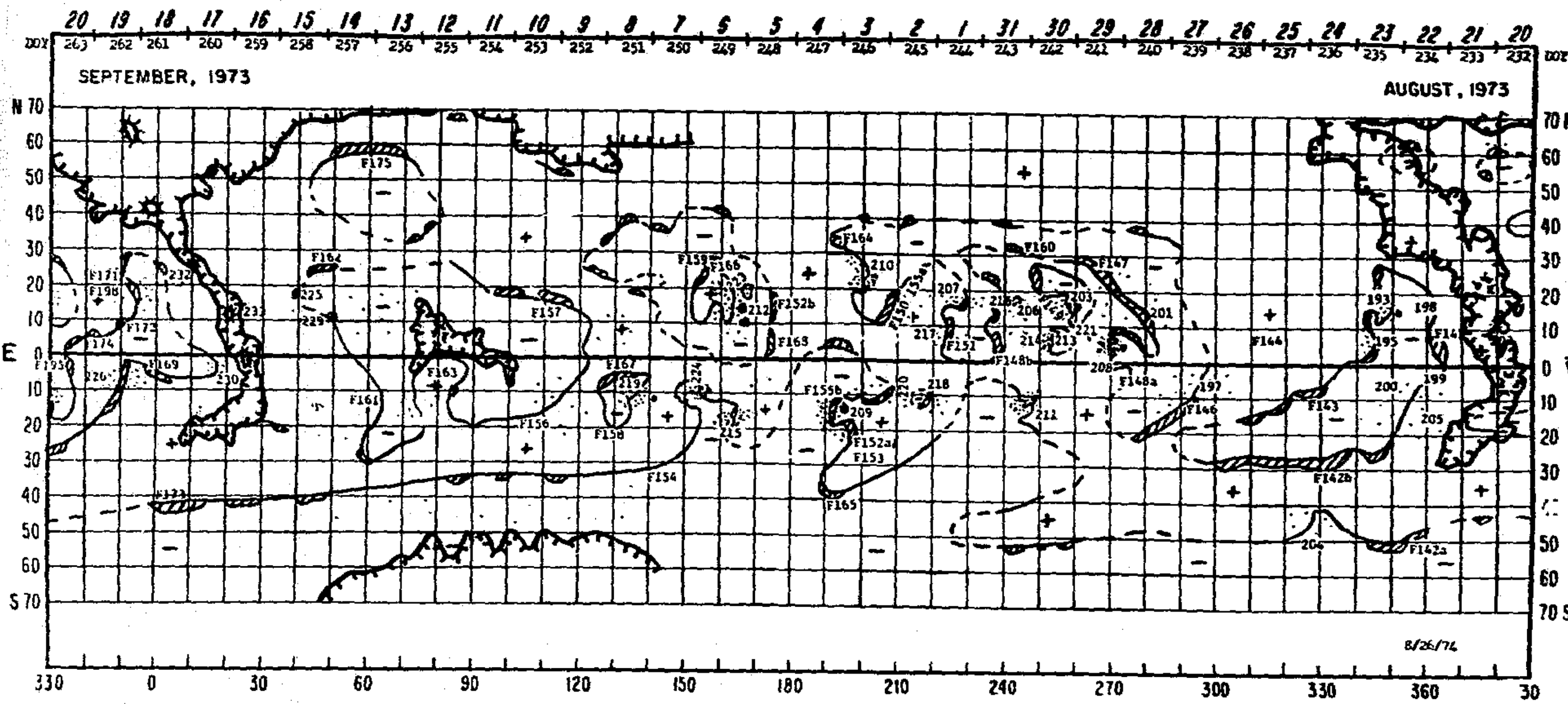

ROTATION NO. 1605 (AUGUST 22 - SEPTEMBER 18)

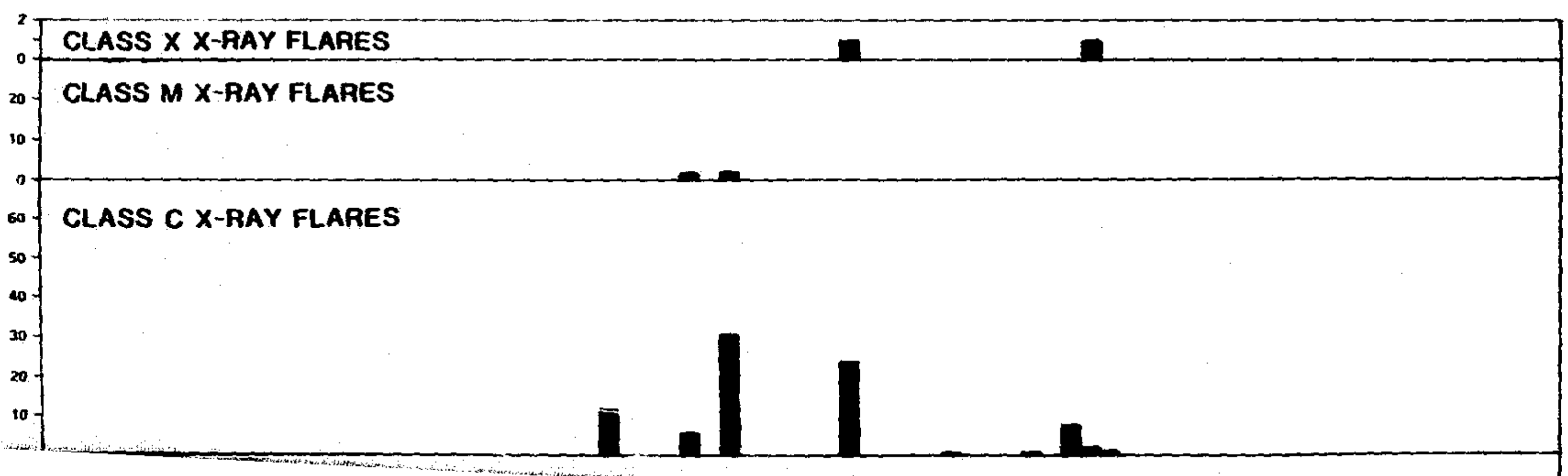


FOLDOUT FRAME

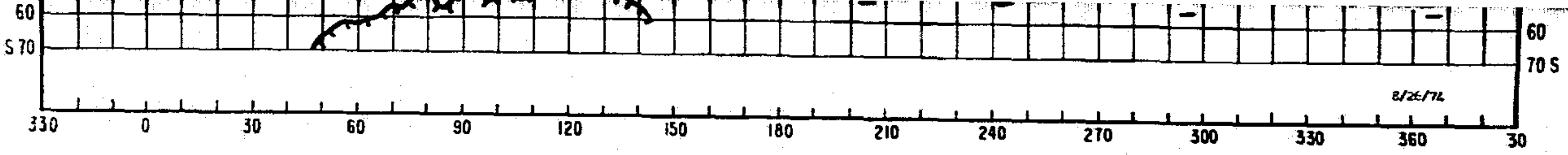


UT FRAME

ROTATION NO. 1605 (AUGUST 22 - SEPTEMBER 18)

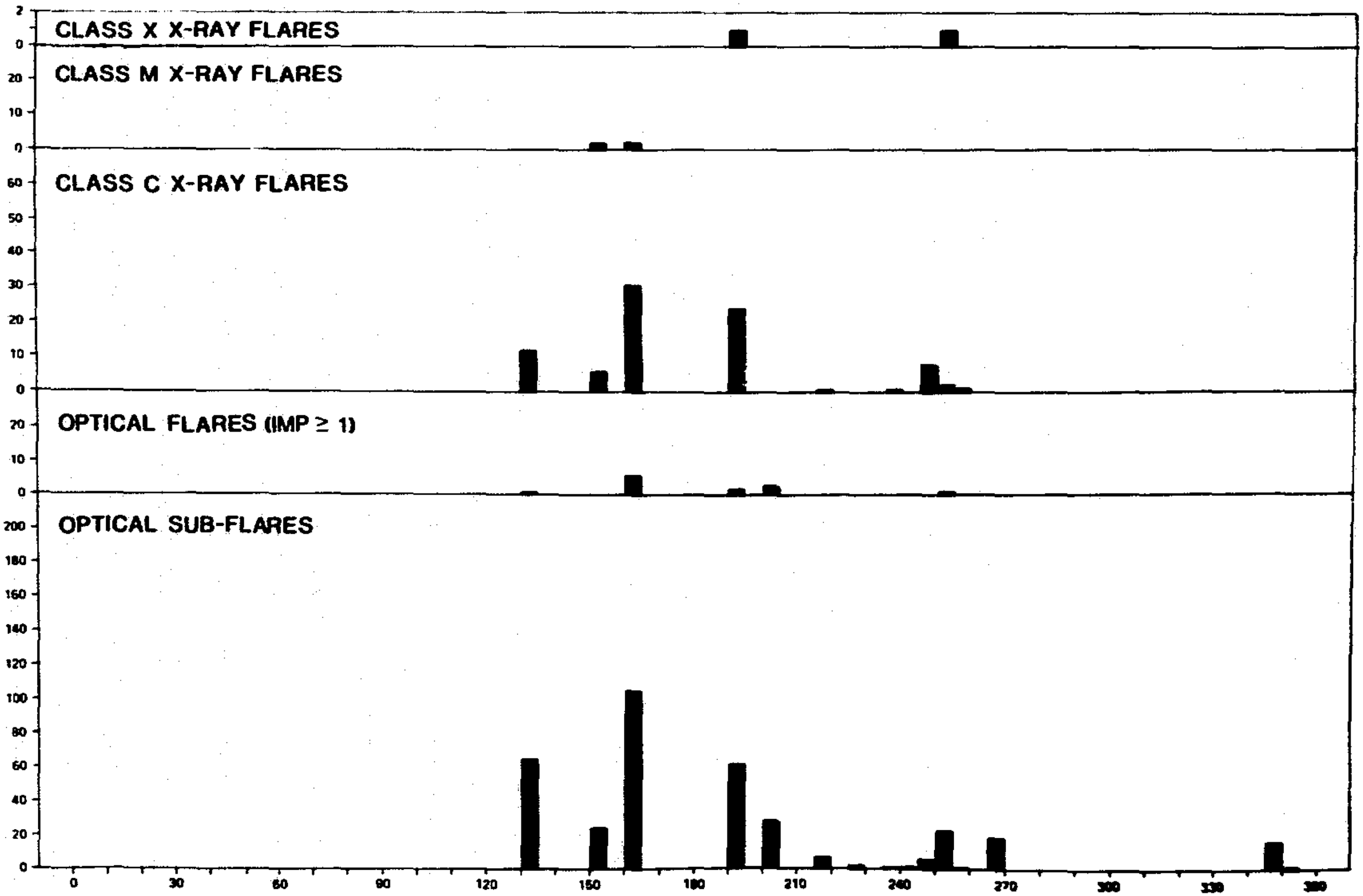


FOLDOUT FRAME 2

Figure 5. Hα synoptic chart with coronal hole boundaries aligned with flare activity histogram for Carrington rotation 1605.

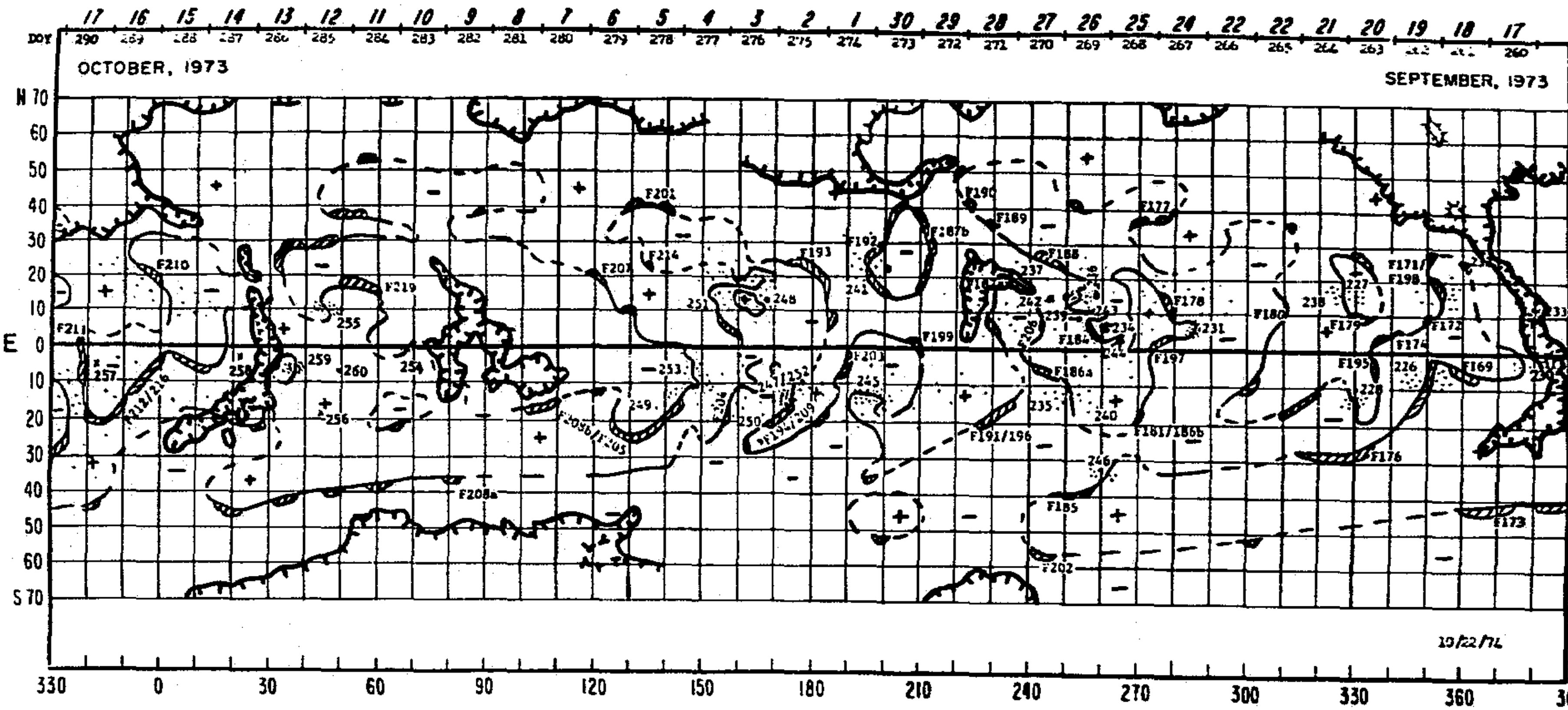


FOLDOUT FRAME

ROTATION NO. 1606 (SEPTEMBER 18 - OCTOBER 15)

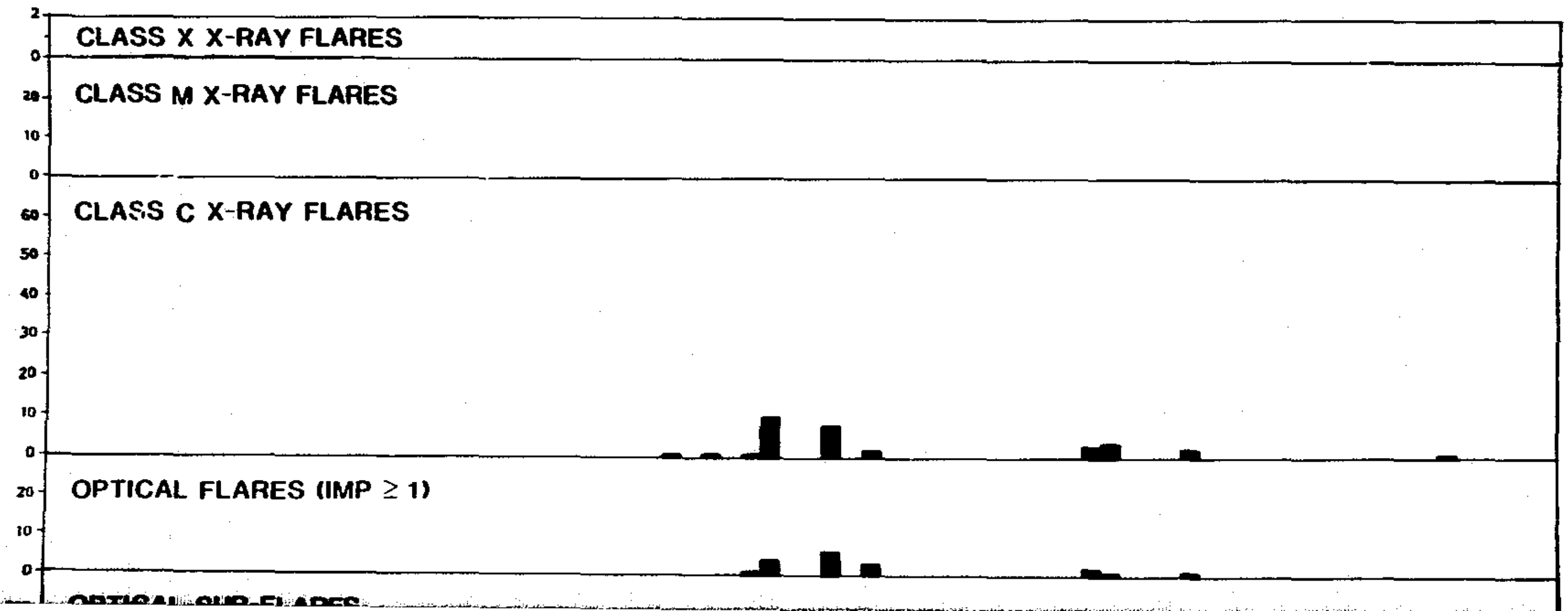

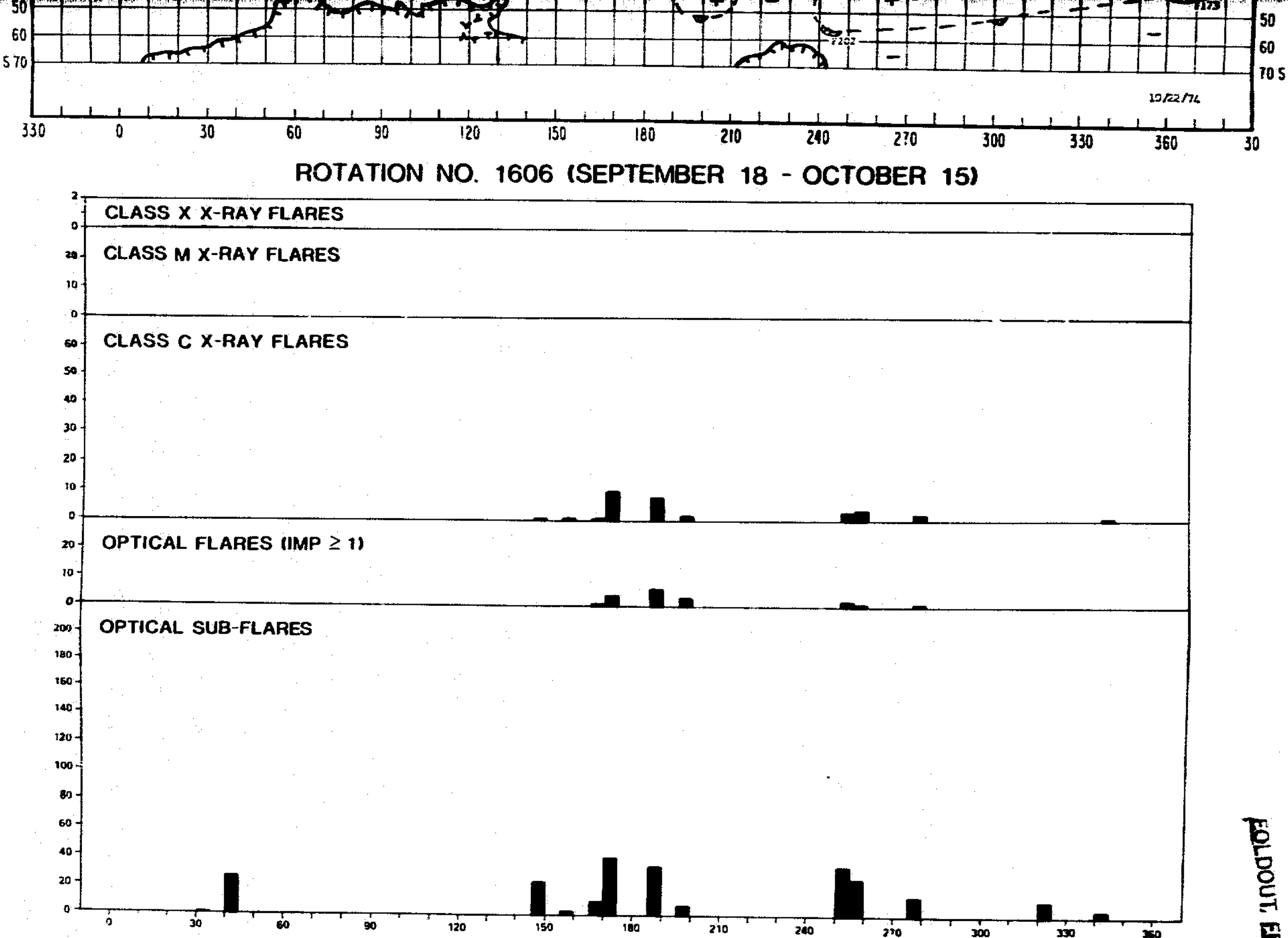


Figure 6. Hα synoptic chart with coronal hole boundaries aligned with flare activity histogram for Carrington rotation 1606.

FOLDOUT FRAME

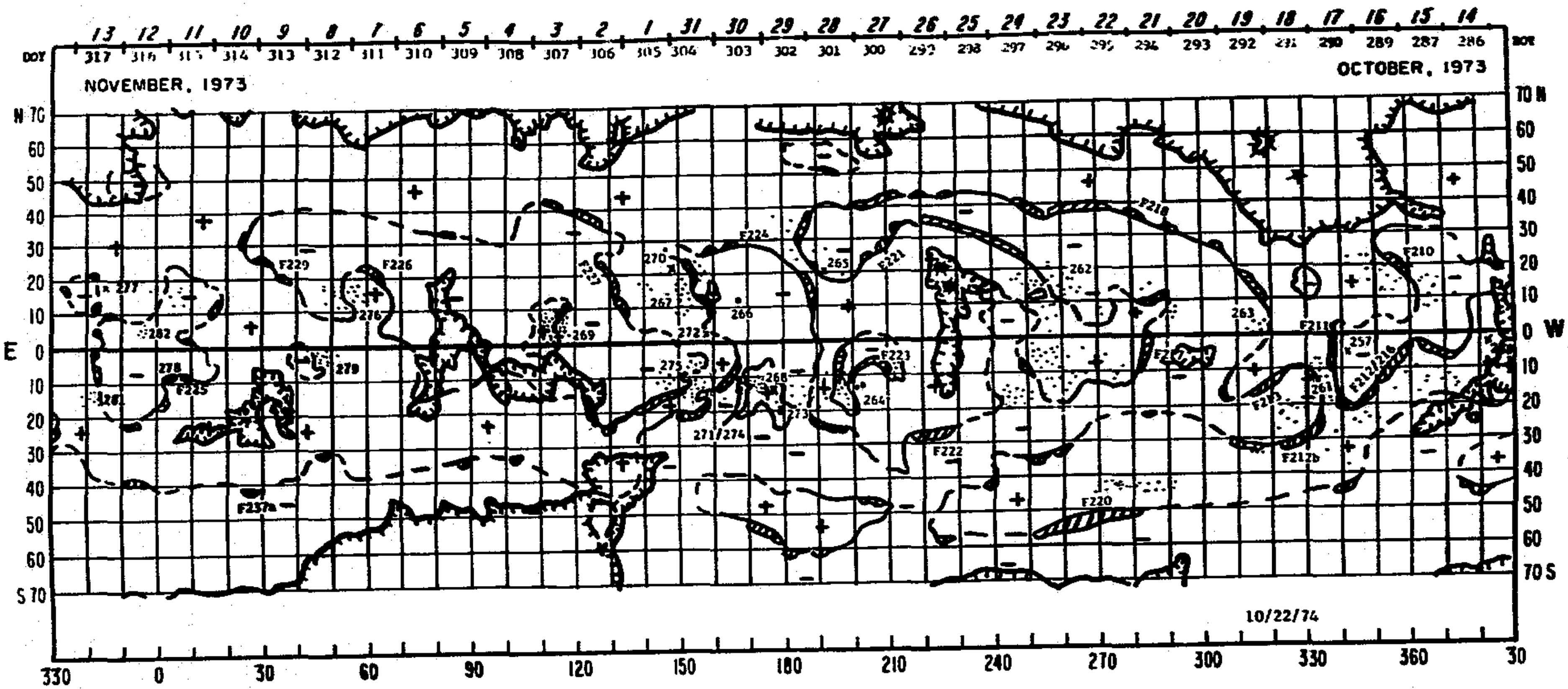


## ROTATION NO. 1607 (OCTOBER 15 - NOVEMBER 12)

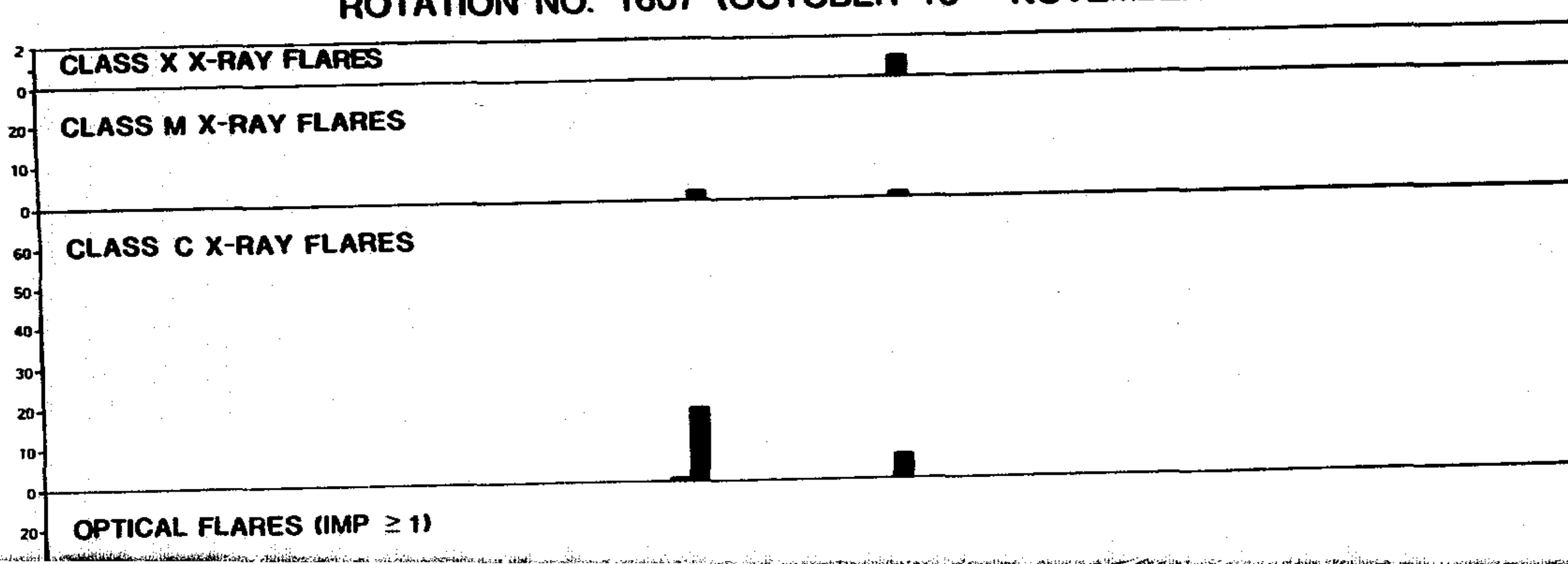

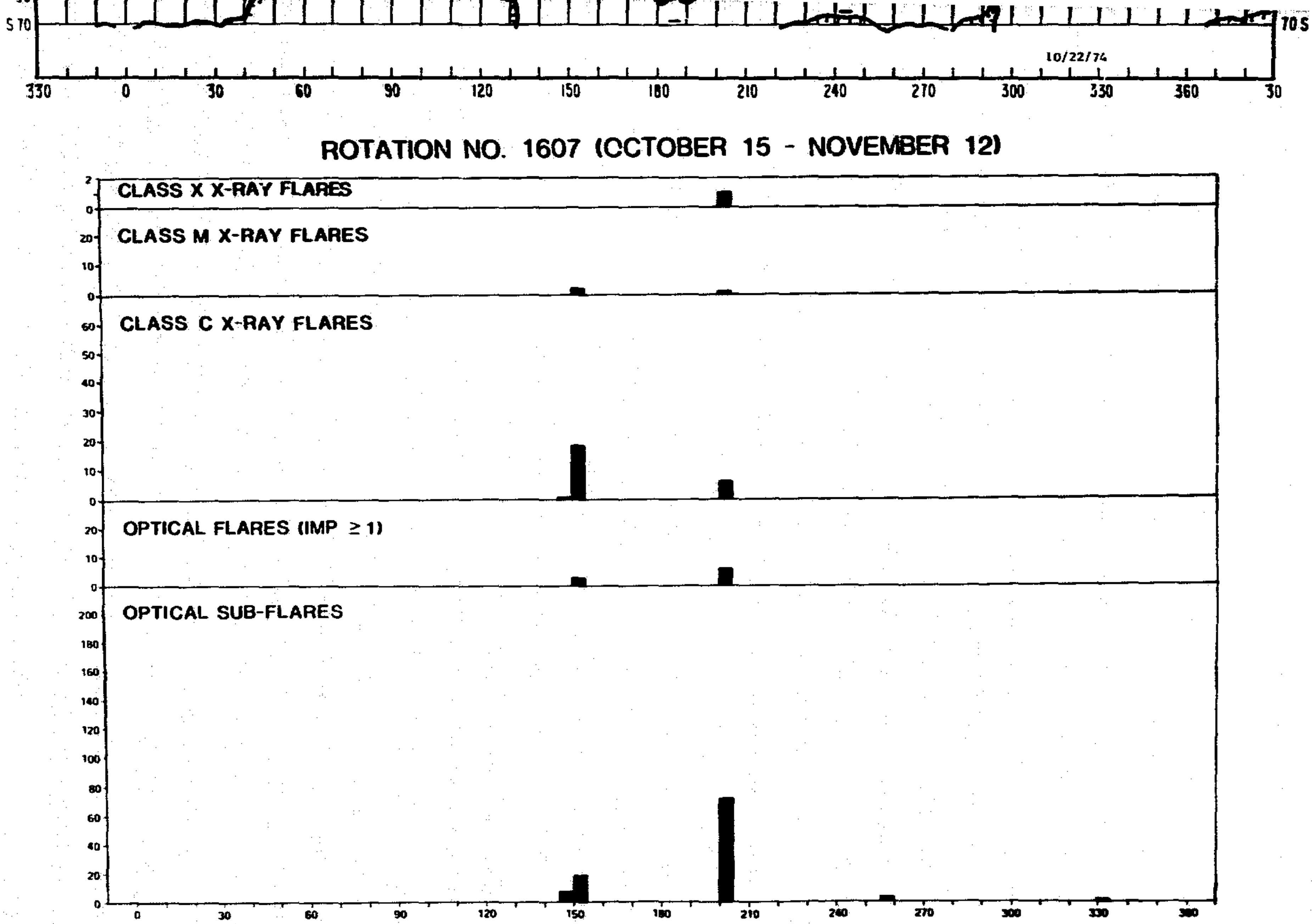


Figure 7. Hα synoptic chart with coronal hole boundaries aligned with flare activity histogram for Carrington rotation 1607.

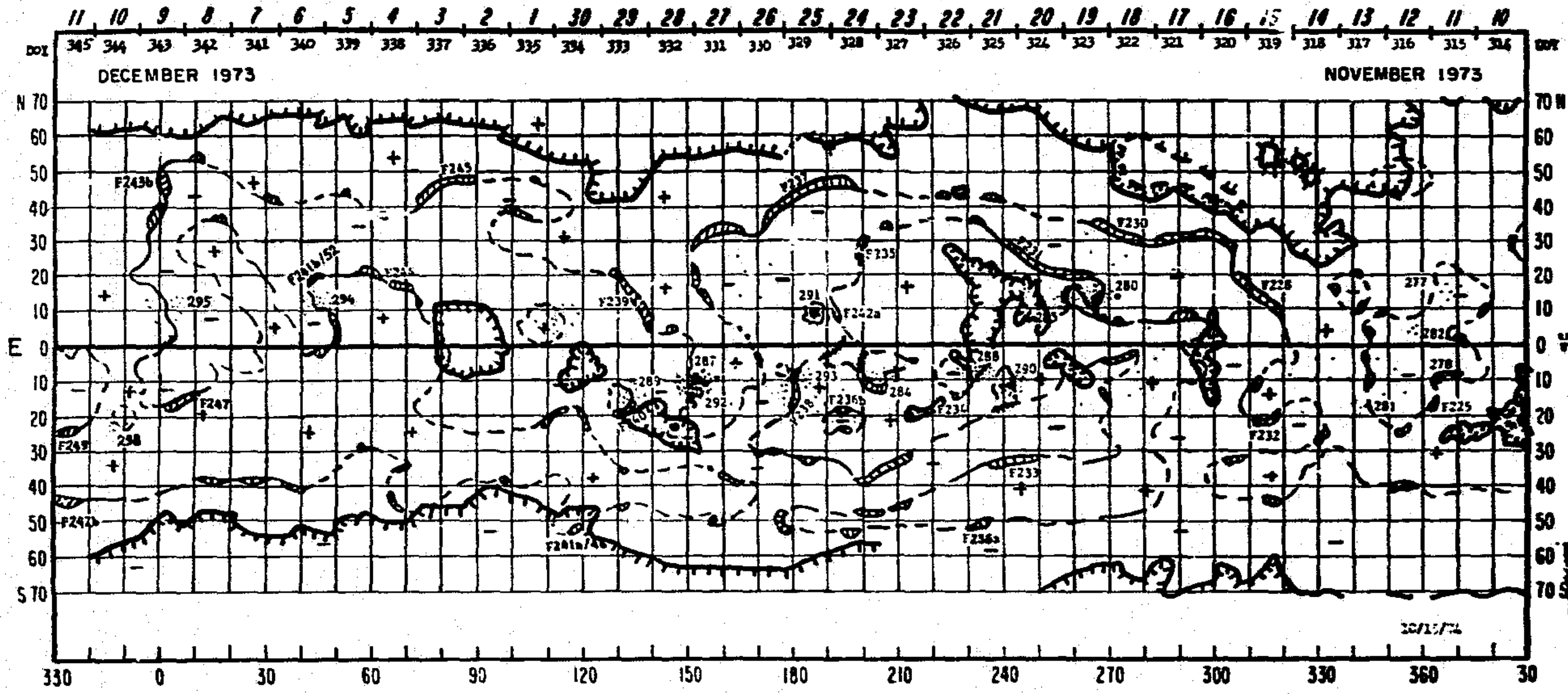


ROTATION NO. 1608 (NOVEMBER 12 - DECEMBER 9)

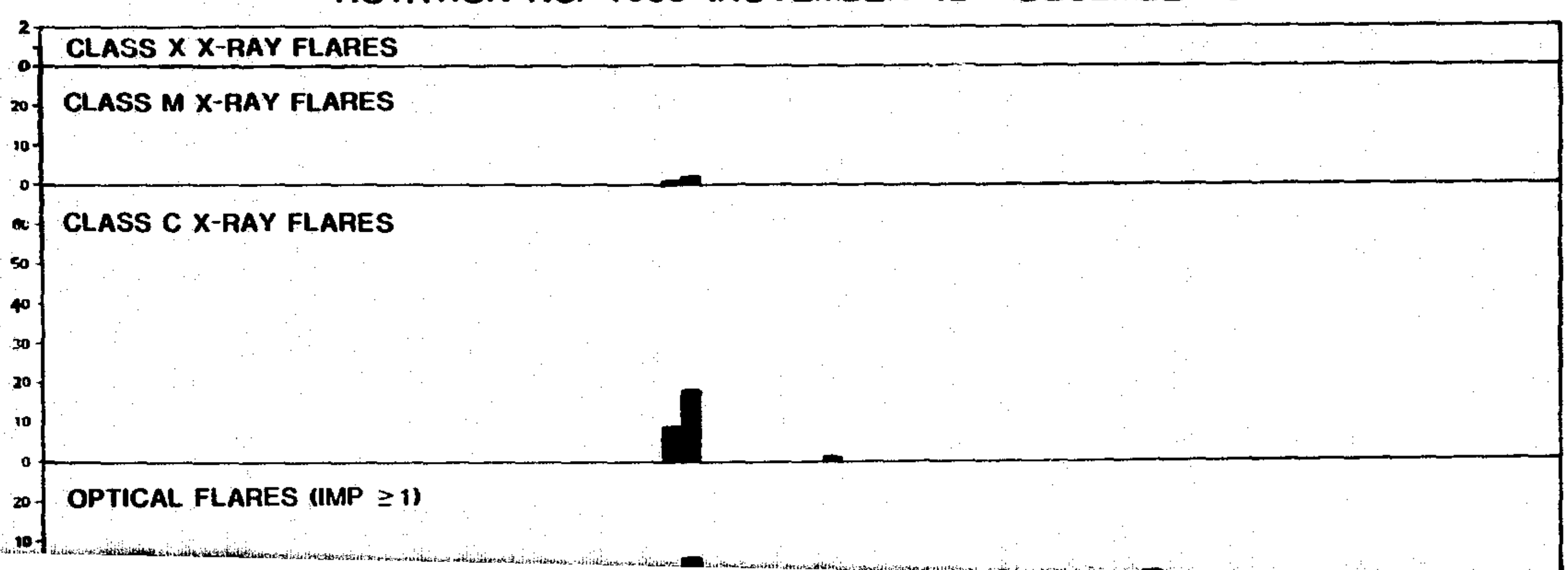


FOLDOUT FRAME

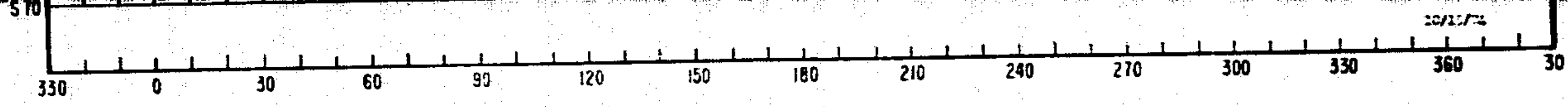

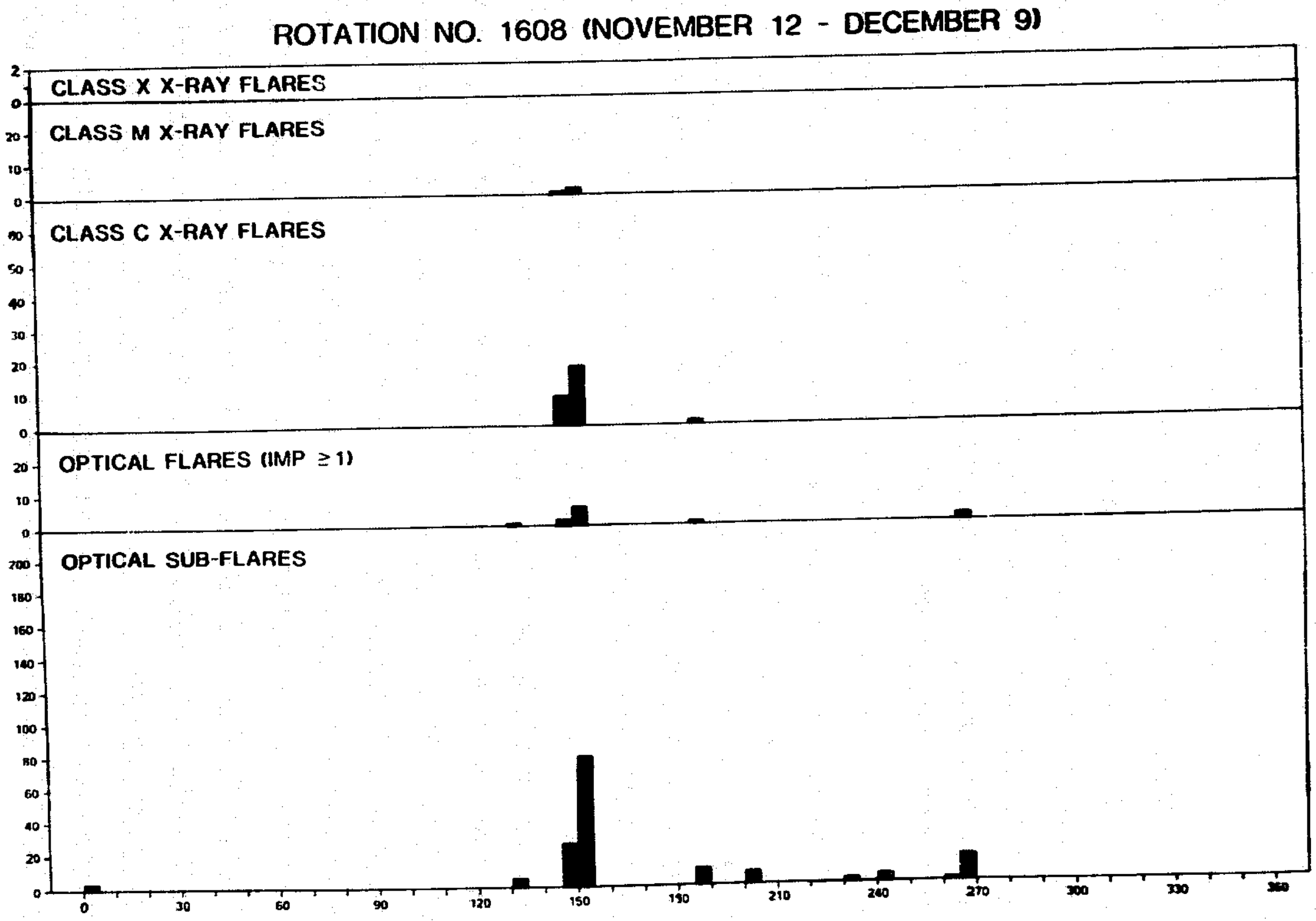


Figure 8. Hα synoptic chart with coronal hole boundaries aligned with flare activity histogram for Carrington rotation 1608.

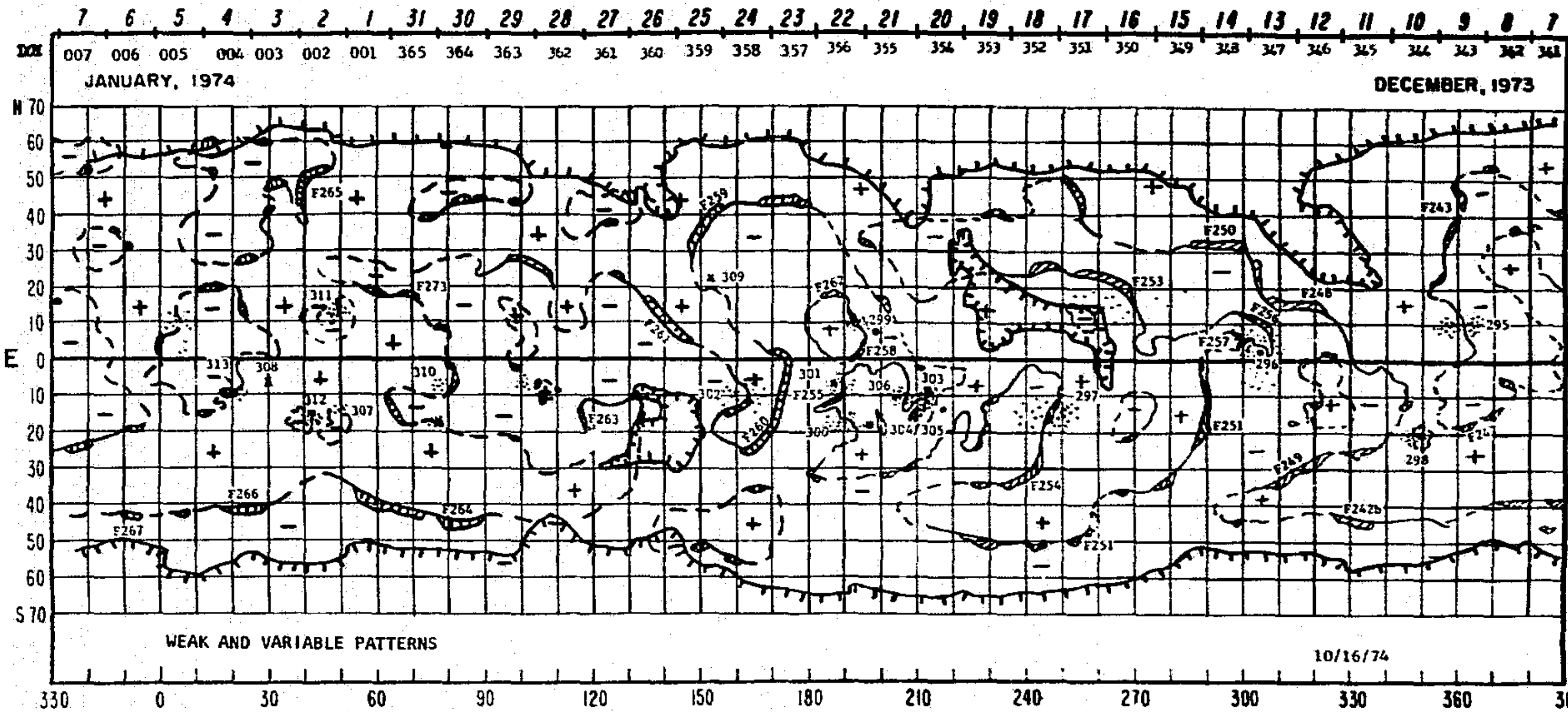


ROTATION NO. 1609 (DECEMBER 9 - JANUARY 5)

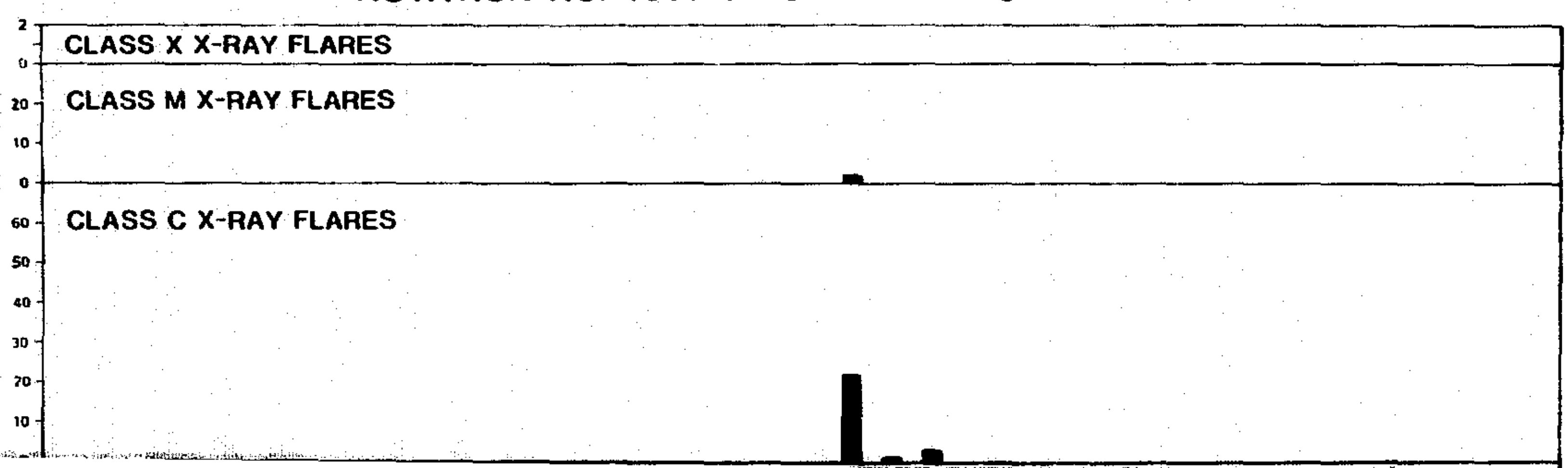


FOLDOUT FRAME

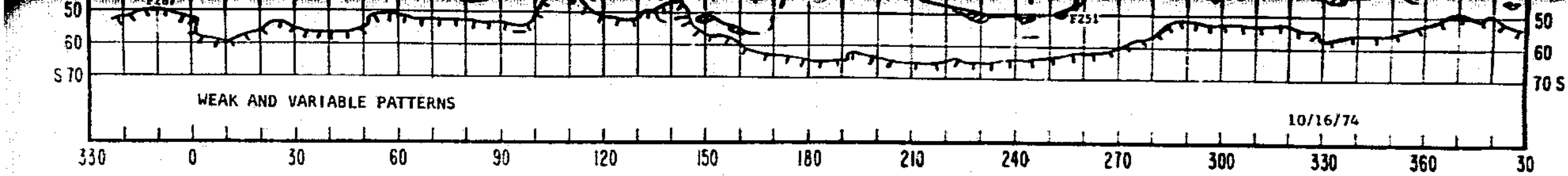


ROTATION NO. 1609 (DECEMBER 9 - JANUARY 5)

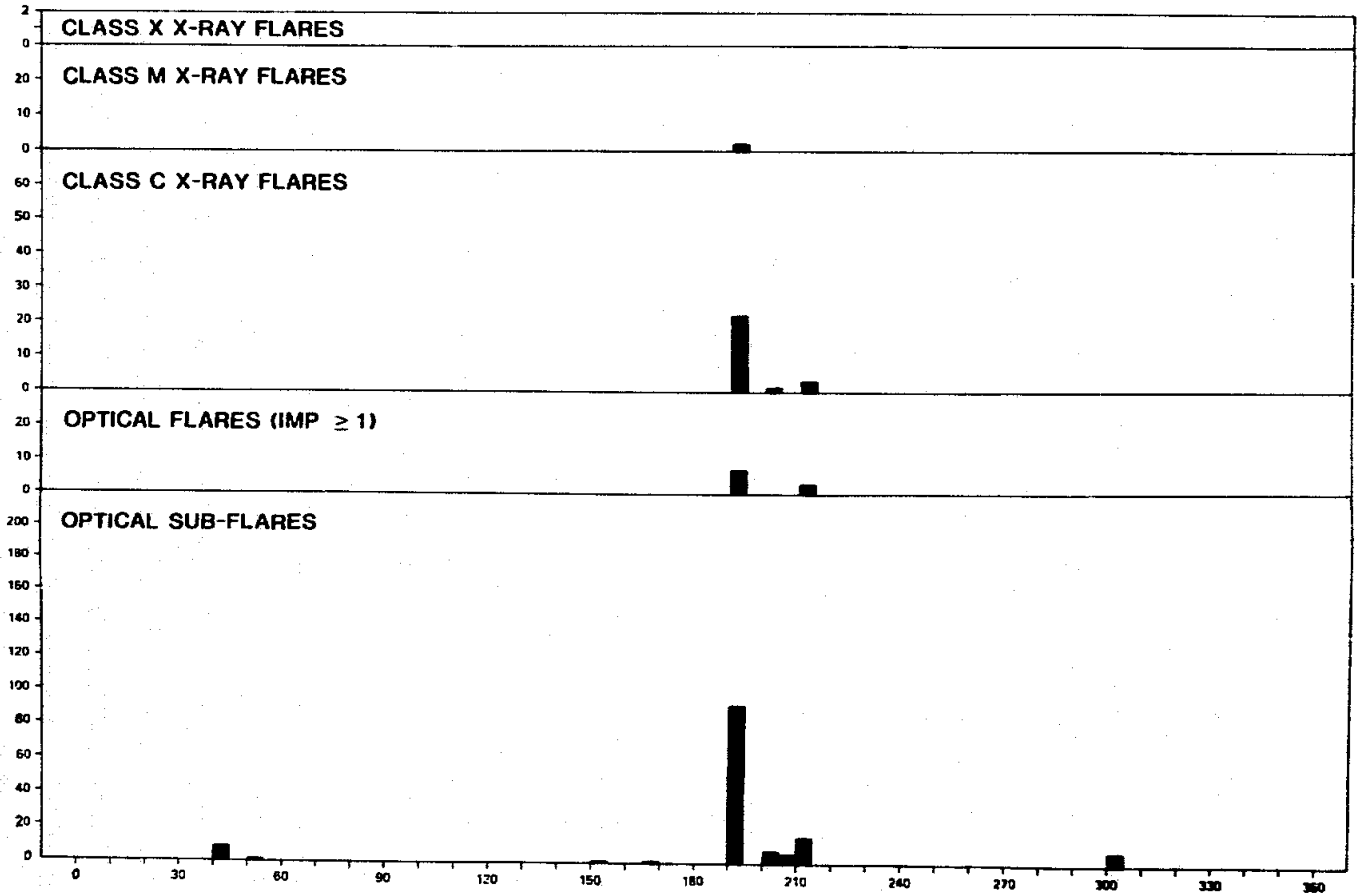


FOLDOUT FRAME 2

Figure 9. Hα synoptic chart with coronal hole boundaries aligned with flare activity histogram for Carrington rotation 1609.

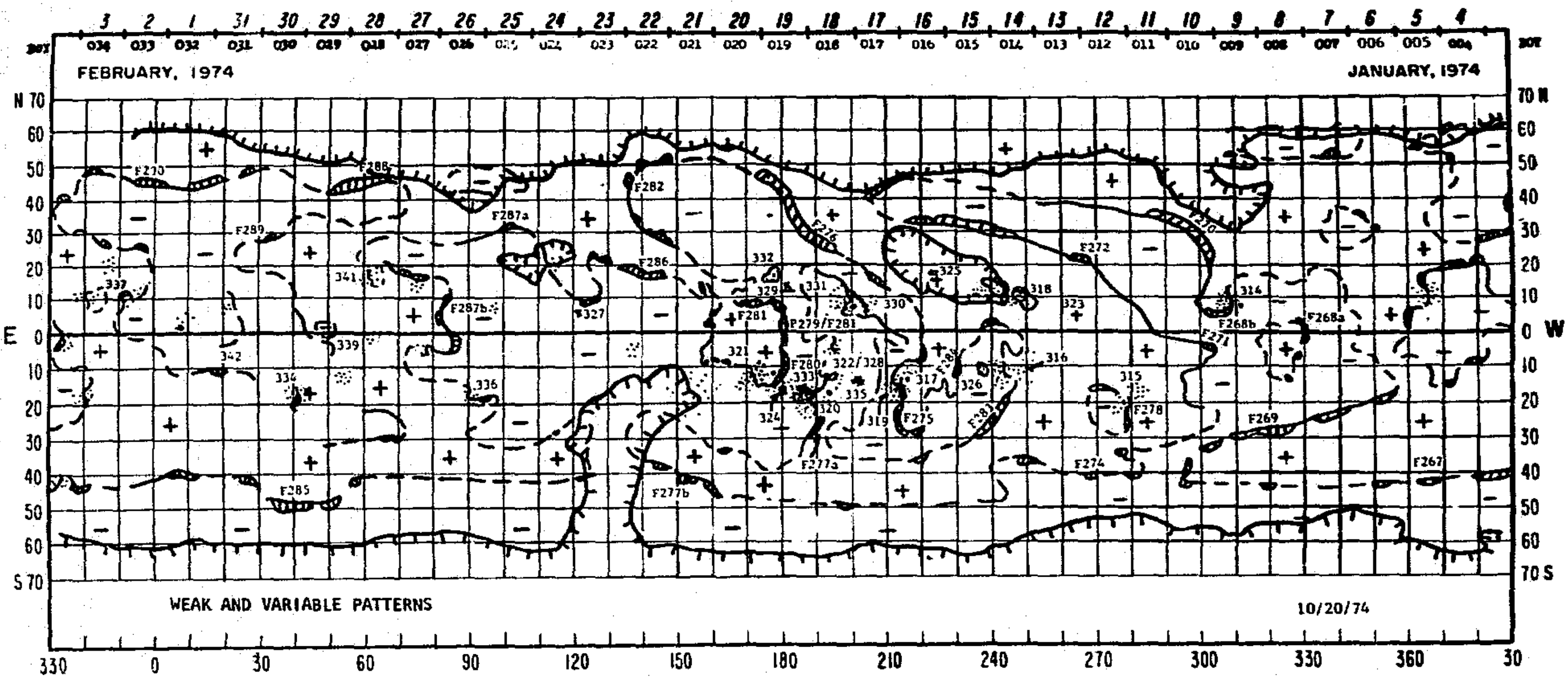


ROTATION NO. 1610 (JANUARY 5 - FEBRUARY 2)

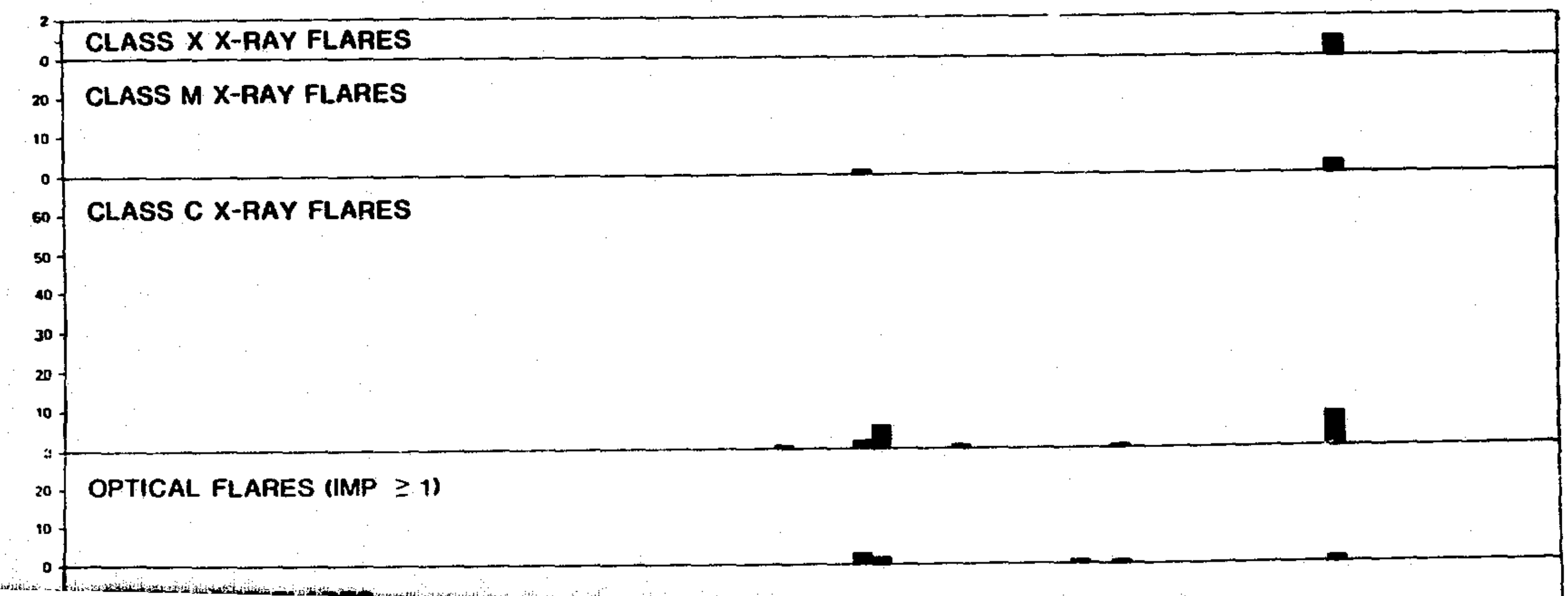


FOLDOUT FRAME 1

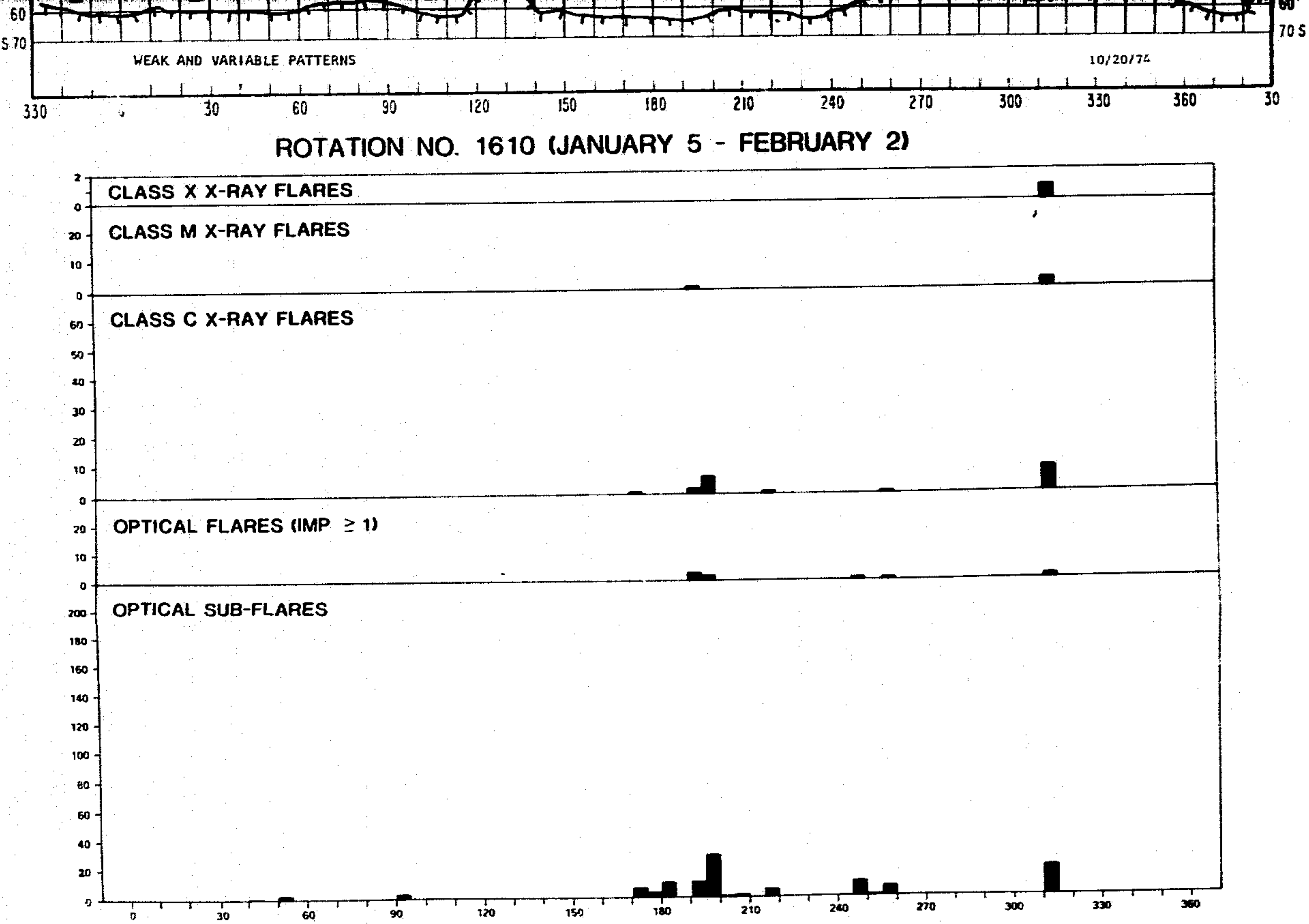


Figure 10. Hα synoptic chart with coronal hole boundaries aligned with flare activity histogram for Carrington rotation 1610.

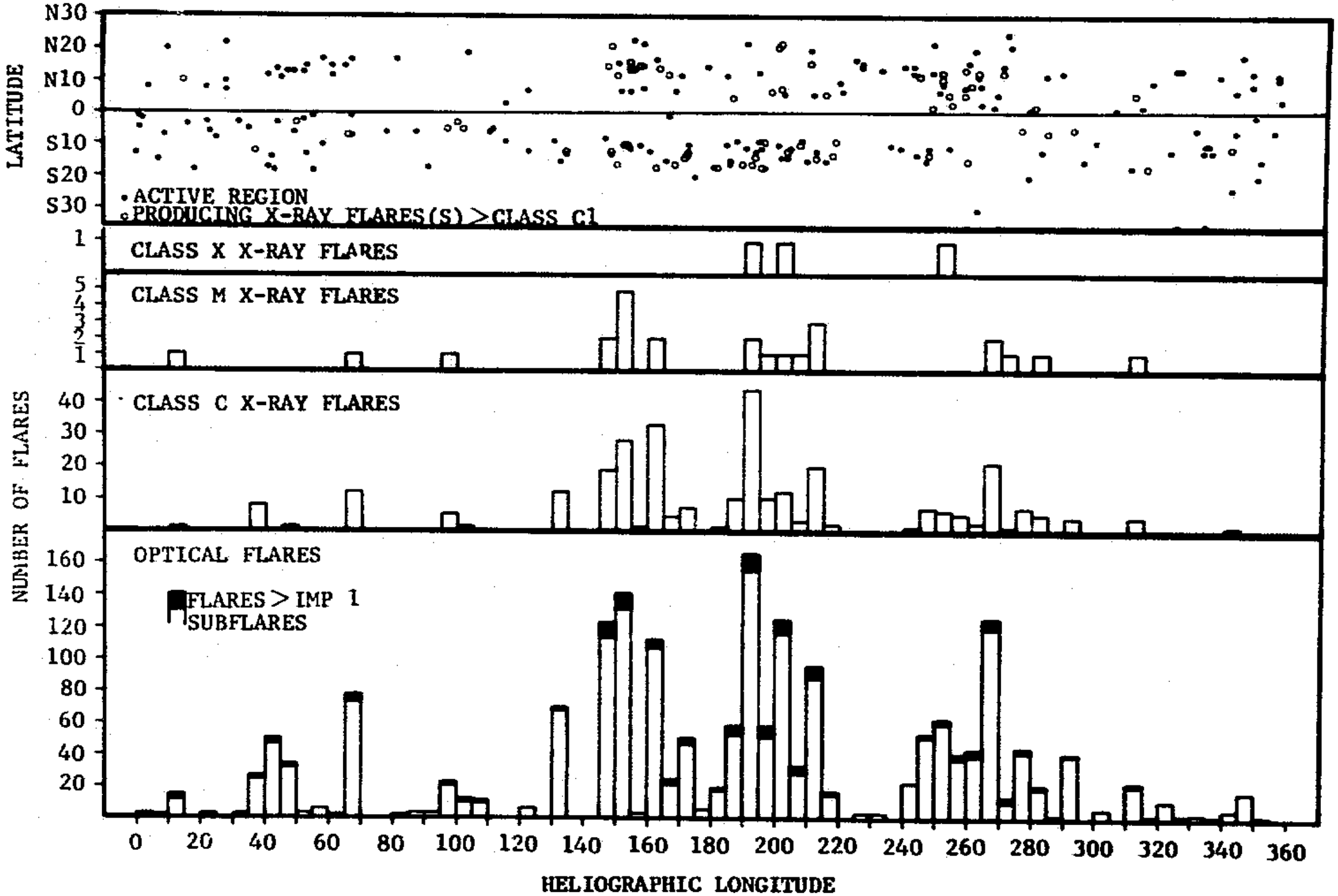


Figure 11. Solar longitudinal distribution of flares and active region positions for the Skylab period.

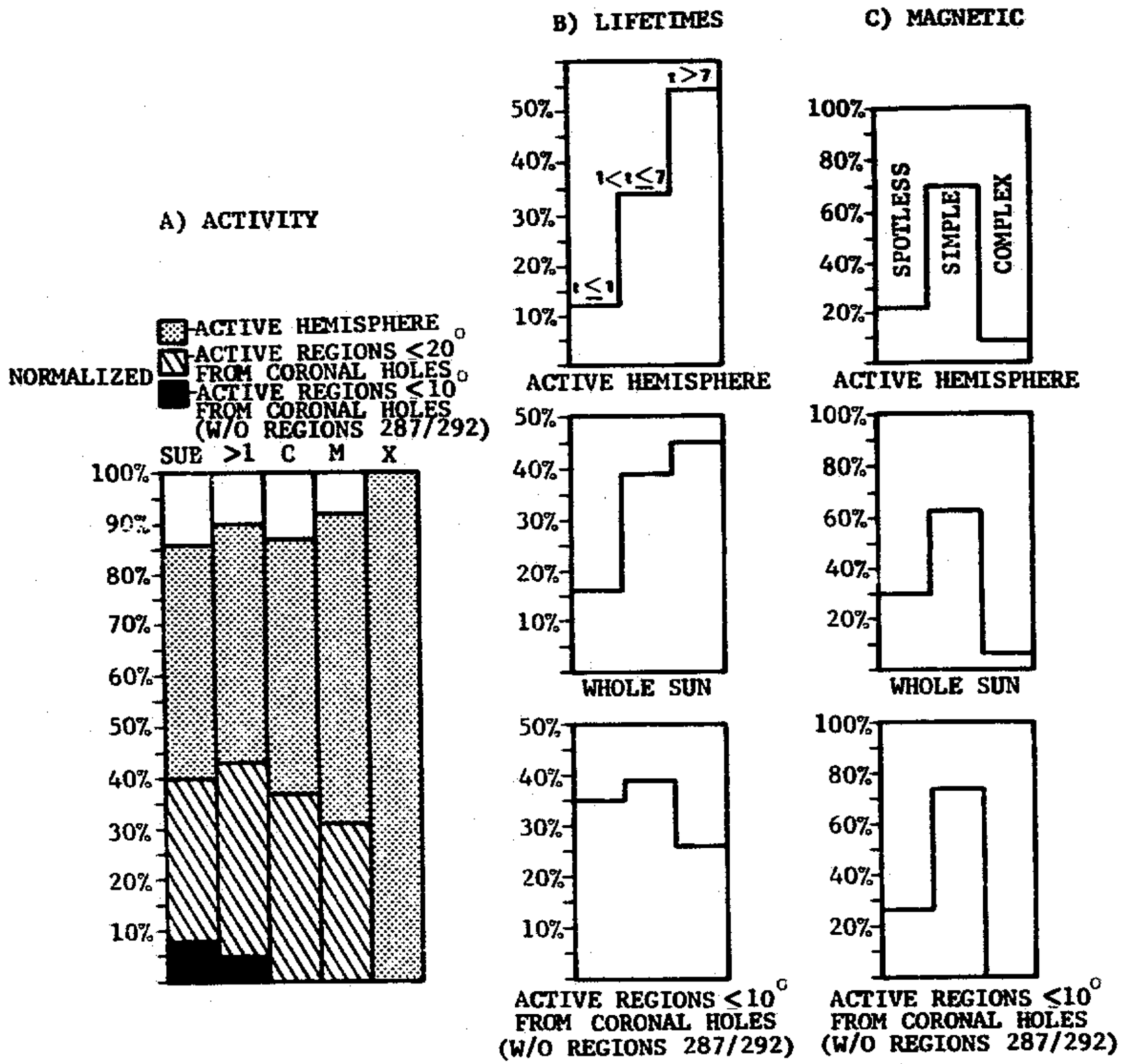


Figure 12. Flare activity production, lifetimes, and magnetic classifications for various subsets of active regions observed during Skylab.

## TABLE 1. FLARE ACTIVITY PRODUCTION, LIFETIMES, AND MAGNETIC CLASSIFICATIONS FOR VARIOUS SUBSETS OF ACTIVE REGIONS OBSERVED DURING SKYLAB

| | All Skylab Active Regions | Active Longitudes (136° - 315°) | Active Regions ≤ 20° from CHs | Active Regions ≤ 10° from CHs | Active Regions ≤ 10° from CHs **Without** 287/292 |
|---|---|---|---|---|---|
| **Flare Activity** | | | | | |
| Number of Active Regions | 233 | 136 (58%) | 73 (31%) | 33 (14%) | 31 (13%) |
| Number of Subflares | 1784 | 1535 (86%) | 412 (23%) | 138 (7%) | 33 (2%) |
| Number of IMP ~ 1 Flares | 104 | 94 (90%) | 24 (23%) | 9 (9%) | 1 (1%) |
| Number of Class C X-Ray Flares | 294 | 257 (87%) | 58 (20%) | 27 (9%) | 0 (0%) |
| Number of Class M X-Ray Flares | 24 | 22 (92%) | 4 (17%) | 3 (13%) | 0 (0%) |
| Number of Class X X-Ray Flares | 3 | 3 (100%) | 0 (0%) | 0 (0%) | 0 (0%) |
| **Lifetimes** | | | | | |
| Active Regions ≤ 1 Day | 16% | 12% | 25% | 33% | 35% |
| Active Regions > 1 and ≤ 7 Days | 39% | 34% | 38% | 37% | 39% |
| Active Regions > 7 Days | 45% | 54% | 37% | 30% | 26% |
| **Magnetic Classifications** | | | | | |
| Regions Without Sunspots | 31% | 22% | 30% | 24% | 26% |
| Simple ($\alpha$, $\beta$) | 63% | 70% | 66% | 73% | 74% |
| Complex ($\beta\gamma$, $\beta\gamma\Delta$) | 6% | 8% | 4% | 3% | 0% |

# REFERENCES


1. Dodson, H. W. and Hedeman, E. R.: Comments on the Course of Solar Activity During the Declining Phase of Solar Cycle 20 (1970-74). Solar Phys., vol. 42, 1975.

2. Hildner, E., Gosling, J. T., MacQueen, R. M., Munro, R. H., Poland, A. I., and Ross, C. L.: Frequency of Coronal Transients and Solar Activity. Solar Phys., vol. 48, 1976.

3. Golub, L., Krieger, A. S., and Vaiana, G. S.: Observation of Spatial and Temporal Variations in X-Ray Bright Point Emergence Patterns. Solar Phys., vol. 50, 1976.

4. Bohlin, J. D.: The Physical Properties of Coronal Holes. Physics of Solar Planetary Environments (D. J. Williams, ed.), Vol. 1, American Geophysical Union, 1976.

5. McIntosh, P. S.: H-alpha Synoptic Charts of Solar Activity for the Period of Skylab Observations May, 1973-March, 1974. World Data Center A for Solar-Terrestrial Physics, Report UAG-40, 1975.

6. Bohlin, J. D. and Rubenstein, D. M.: Synoptic Maps of Solar Coronal Hole Boundaries Derived from He II 304A Spectroheliograms from the Manned Skylab Missions. World Data Center A for Solar-Terrestrial Physics, Report UAG-51, 1975.

7. McIntosh, P. S., Krieger, A. S., Nolte, J. T., And Vaiana, G. S.: Association of X-Ray Arches with Chromospheric Neutral Lines. Solar Phys., vol. 49, 1976.

8. Nolte, J. T., Krieger, A. S., Timothy, A. F., Vaiana, G. S., and Zombeck, M. V.: An Atlas of Coronal Hole Boundary Positions May 28 to November 21, 1973. American Science and Engineering Preprint ASE-3787, 1975.

9. Hirman, J. W., Losey, R. M., and Heckman, G. R.: A Compilation of Solar Flares Reported During the Skylab Mission. NOAA Technical Memorandum ERL SEL-49, 1977.

10. Bohlin, J. D.: An Observational Definition of Coronal Holes. Coronal Holes and High Speed Wind Streams (J. B. Zirker, ed.), Colorado Assoc. Univ. Press, 1977.

# APPROVAL

## SOLAR ACTIVITY DURING SKYLAB – ITS DISTRIBUTION AND RELATION TO CORONAL HOLES

By David M. Speich, Jesse B. Smith, Jr., Robert M. Wilson, and Patrick S. McIntosh

The information in this report has been reviewed for security classification. Review of any information concerning Department of Defense or nuclear energy activities or programs has been made by the MSFC Security Classification Officer. This report, in its entirety, has been determined to be unclassified.

Anthony C. DeLoach

ANTHONY C. DeLOACH
Chief, Solar Sciences Branch

William C. Snoddy

WILLIAM C. SNODDY
Chief, Solar-Terrestrial Physics Division

Charles A. Lundquist

CHARLES A. LUNDQUIST
Director, Space Sciences Laboratory

☆ U. S. GOVERNMENT PRINTING OFFICE 1978—740-193/364 REGION NO. 4